



Pervasive speleogenetic modification of cave passages by nitrification of biogenic ammonia

Andrew R. Farrant^{a,*}, J. Max Koether^b, Hazel A. Barton^b, Stein-Erik Lauritzen^c,
Christos Pennos^d, Andrew C. Smith^a, Jo White^e, Andrew McLeod^f, Andrew J. Eavis^g

^a British Geological Survey, Keyworth, Nottingham NG12 5GG, United Kingdom

^b Department of Geological Sciences, The University of Alabama, Box 870338, Tuscaloosa, AL 35487, United States of America

^c Department of Earth Science, University of Bergen, Allég. 41, 5007 Bergen, Norway

^d University of Department of Geography, University of Bergen, Fosswinkels gt. 6, 5007 Bergen, Norway

^e Department of Chemical and Biological Sciences, University of Huddersfield, Queensgate, Huddersfield HD1 3DH, United Kingdom

^f 2 Greta Cottages, Ingleton, Carnforth LA6 3EZ, United Kingdom

^g Tides Reach, Redcliff Road, Hessle, Hull HU13 0HA, United Kingdom

ARTICLE INFO

Keywords:

Biogeomorphology
Speleogenesis
Karst
Geomicrobiology

ABSTRACT

It has long been known that guano deposits from animals in caves can cause localised biogenic modification through a combination of acidity and altered environmental conditions, such as increased humidity and CO₂. Geomorphological and geochemical evidence from the caves in the Gunung Mulu National Park, Sarawak, suggest this biogenic overprint may be far more widespread than previously thought due to microbial metabolic activity. Based on our observations, we propose a novel method of secondary cave enlargement by the conversion of highly soluble ammonia gas released by bat and swiftlet guano to NO_x on surfaces by microbial ammonia oxidation. Our data suggest this activity produces aggressive nitric acid solutions on moist cave walls, accelerating limestone dissolution. This previously undescribed cave enlargement process has potentially profound geomorphological implications, as the original passage morphologies (which are used to interpret speleogenesis and landscape evolution) are erased and replaced with a distinctive suite of biogenic corrosion features. Such findings significantly alter our understanding of post-speleogenetic modification and secondary enlargement of caves in tropic environments.

1. Introduction

Caves are important repositories of geomorphological information. Their morphology, sediments, and speleothems can provide evidence for landscape evolution, paleoclimatic and environmental change (Palmer, 2007; Ford and Williams, 2007). There is an increasing recognition that biological processes have a significant impact on the formation of geomorphological features (Viles, 2012), including caves and karst, a concept termed zoogeomorphology (Butler, 1995; Viles, 2020). In particular, there is a growing appreciation of the role of microorganisms in the production of carbonic and other acids that aid speleogenesis (Barton and Northup, 2007; Jones and Northup, 2021).

Many caves in tropical and temperate environments are known to host large populations of bats and cave-dwelling swiftlets, with extensive guano deposits that provide the energy source for complex

subterranean ecosystems. Previous studies have highlighted how bird and bat guano can influence cave geomorphology and secondary speleogenetic enlargement through biogenic corrosion (Tarhule-Lips and Ford, 1998; Lundberg and McFarlane, 2012; Audra et al., 2016; Cailaud, 2017; Dandurand et al., 2019; Sala et al., 2023). Many authors have highlighted the biogenic alteration of the host bedrock beneath guano deposits through the production of phosphoric acid (Audra et al., 2019; Dandurand et al., 2019), which results in a heavily corroded bedrock surface, including pinnacles, pedestals, fins and other forms of rock-sculpturing known as karren (Audra et al., 2016). The leaching of phosphoric acid (and potentially other acids) from the guano also leads to the formation of authigenic minerals and alteration crusts, with the common formation of phosphate-rich minerals, including hydroxylapatite, brushite, ardealite, taranakite and variscite, along with many other rarer minerals (Audra et al., 2019).

* Corresponding author.

E-mail address: arf@bgs.ac.uk (A.R. Farrant).

<https://doi.org/10.1016/j.geomorph.2025.109822>

Received 16 December 2024; Received in revised form 14 April 2025; Accepted 6 May 2025

Available online 9 May 2025

0169-555X/© 2025 The Authors. Published by Elsevier B.V. This is an open access article under the CC BY license (<http://creativecommons.org/licenses/by/4.0/>).

Lundberg and McFarlane (2012) identified a possible zoogeomorphic origin for dissolutional features in the Gomantong Caves, Borneo. They suggested roosting birds and bats enhanced condensation corrosion through a combination of exhaled CO₂ and moisture, and an increased local temperature from the body of the animal. Similar structures known as bell holes—small blind cylindrical sub-vertical bell-shaped holes a few centimetres to tens of centimetres in depth—occur in the roof of many tropical caves (Lundberg and McFarlane, 2009, 2012; James, 2011; Dandurand et al., 2019). These are believed to form as a bat urinates during its approach to the roost (Dandurand et al., 2019).

Mammalian urine is slightly acidic (pH 4.6–7.0) and is broken down by bacterial urease, to produce ammonia and CO₂ (McFarlane et al., 1995). These biogenic, post-speleogenetic corrosion processes (described by Lundberg and McFarlane, 2012; Audra et al., 2016, 2019; Dandurand et al., 2019; Barriquand et al., 2021; and Sala et al., 2023) are generally restricted to the immediate locale around roosts but can occur on a significant scale. For example, Lundberg and McFarlane (2012), suggested as much as 70–95 % of the volume of the Gomantong Caves may be due to animal activity and zoogeomorphic processes. In their model, bat-driven subaerial dissolution leads to biogenically-induced collapse,

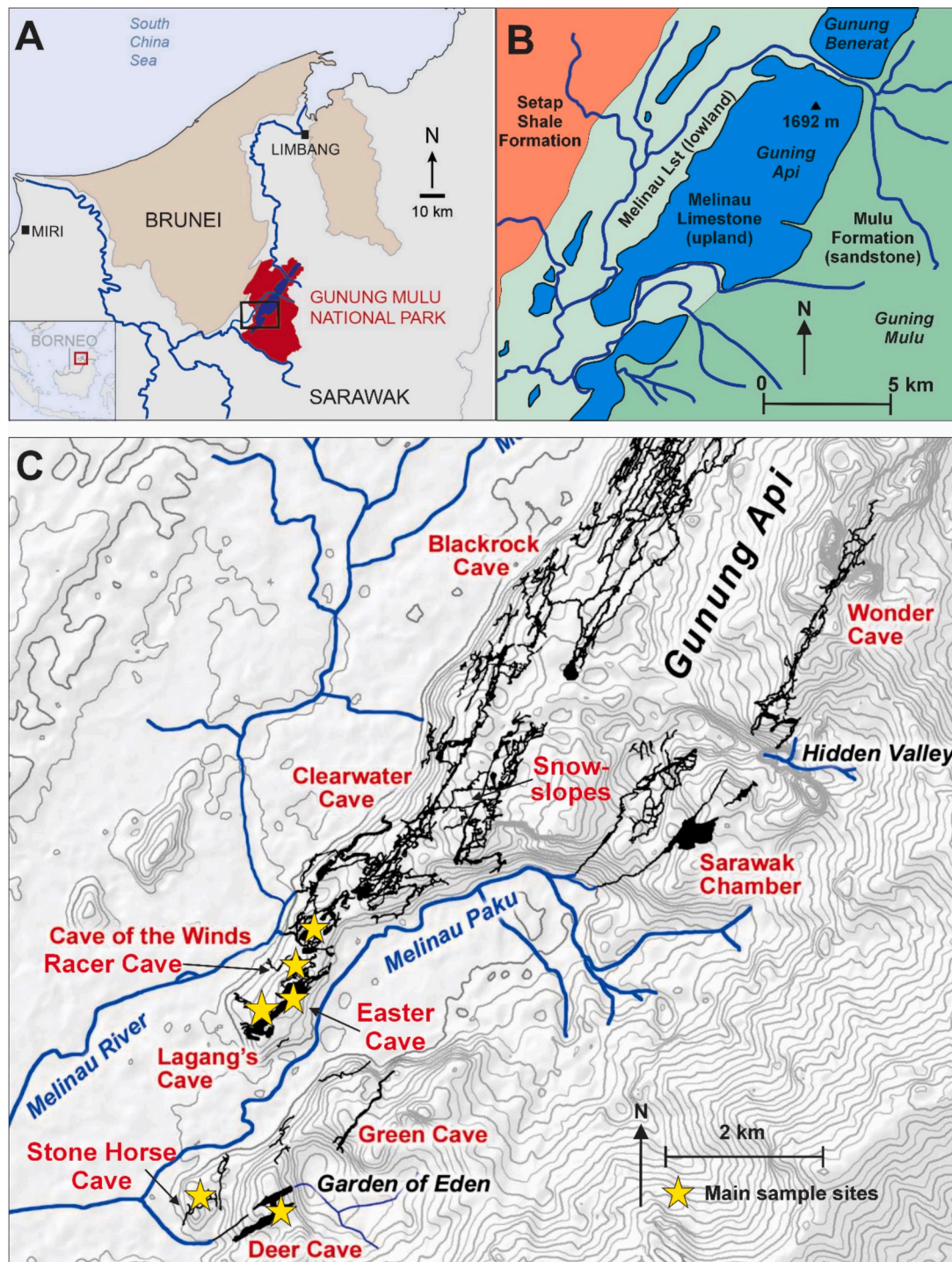


Fig. 1. A. Location of the Gunung Mulu National Park in Sarawak. B. Geologic map of the park, showing the Melinau Limestone ridge. C. The southern part of the park, with the major caves highlighted. Key sample sites are highlighted.

and subsequent sub-cutaneous removal of limestone.

Southeast Asia is rich in limestone terrains that host caves with significant bat and bird populations. Geomorphological features in the extensive cave systems of the Gunung Mulu National Park in Sarawak (Fig. 1) suggest post-abandonment passage modifications and speleothem corrosion induced by animal activity may be more significant than previously realised. The evidence presented here suggests that the impact of bat and bird guano can extend to entire cave systems, leading to a wholesale alteration of passage morphology, with major implications on how the cave passage geomorphology is interpreted. These observations suggest that the mechanism for the observed corrosion cannot be simply due to direct dissolution by guano-derived leachates, urine, or locally enhanced condensation corrosion due to increased CO₂ and moisture. Rather a more pervasive dissolution process appears to be in action through the microbial interconversion of the N cycle, facilitated by gaseous exchange of ammonia through the caves, which can account for the largescale and widespread geomorphological features observed.

2. Geologic setting

The Gunung Mulu National Park is located in equatorial northeast Sarawak, Malaysia, 180 km from the coast. The region can be divided into three distinct morphological units (Fig. 1). The Gunung Mulu uplands (maximum elevation 2377 m) are developed on coarse sandstones of the Mulu Formation. Immediately to the northwest is the rugged, maturely karstified ridge of Gunung Api (1750 m) and Gunung Benerat (1858 m), separated by the Melinau Gorge. This ridge is composed of the massive upper Eocene–lower Miocene Melinau Limestone Formation (James, 1984; Wannier, 2009), which dips at up to 60°–70° to the northwest, forming the northwestern limb of the Mulu anticline. To the west is the low-lying alluvial plain of the Melinau River, at an elevation of <30 m. This is an erosional feature incised in the limestones and the overlying Setap Shale Formation. Underground drainage through the limestone ridge gives rise to some of the largest and most extensive caves in the world, with a total explored length of over 500 km.

Among the Mulu caves, Clearwater Cave is one of the longest caves in the world, with 255 km of surveyed passage. Clearwater Cave is almost certainly the largest cave by volume with typical passage diameters often in excess of 10 m (far bigger than most long cave systems). The system hosts some of the largest cave chambers in the world, such as Api Chamber. The cave is drained by the Clearwater River at base level, with a stacked vertical sequence of relict cave passages above. The highest (oldest) caves are some 500 m above the present resurgence level with an estimated age of 2.5 million years (Farrant et al., 1995; Farrant et al., 2007; Moseley et al., 2013). The southern end of the Clearwater Cave system links to the Cave of the Winds, Racer Cave and Easter Cave. A group of shorter, mostly relict caves occur in a series of isolated limestone hills in the south of the park. These include Stone Horse Cave and Deer Cave. The latter drains the Garden of Eden valley and is one of the largest cave passages in the world. It hosts a very large colony of several million wrinkle-lipped bats in the roof.

Research by previous expeditions focussed on the geomorphology of the Mulu caves (Smart et al., 1985; Farrant et al., 1995, 2007), which demonstrated that the caves are of epigenic origin, formed by fluvial activity with locally significant paragenetic development and alluviation caused by influxes of sediment (Farrant and Smart, 2011). This has created the distinctive notches and paragenetic canyons seen throughout the Mulu caves.

The large caves of Gunung Mulu National Park are home to some of the largest populations of cave swiftlets in the world. Two species of cave swiftlets are present, the black-nest swiftlet, *Aerodramus maximus*, and the white-nest swiftlet, *Aerodramus fuciphagus*. They are widespread, having been observed to fly and roost throughout the cave system, sometimes kilometres from the nearest entrance. Swiftlets are known to have used some roosting sites for thousands of years (Bird

et al., 2007; Wurster et al., 2017). Bat colonies are also common, with most occurring within 500 m of an entrance.

3. Geomorphological evidence for subaerial post-abandonment dissolution

Dissolutional features, collectively known as speleogens, preserved within caves provide evidence for speleogenetic processes, and allow the geomorphological history of a cave to be deduced. In the Mulu caves, a detailed examination of the cave passage morphology revealed features that suggest the caves continue to undergo subaerial dissolution after abandonment by the formative rivers.

The most common speleogens are scallops, small asymmetric scoop like depressions formed by flowing water (Blumberg and Curl, 1974). Their size is inversely proportional to flow velocity, and their asymmetry records the direction of paleo-flow with the steep part of the scallop profile occurring on the upstream side; they can thus be used to quantify palaeohydrology (Lauritzen, 1982). In the Mulu caves, classic small scallops typically 2–5 cm across are common in the active vadose river passages (Fig. 2) and some of the low-level relict passages; however, scallops are conspicuously absent in many of the higher-level relict passages, where the walls are anomalously smooth. The absence of this feature suggests that there has been sufficient secondary dissolution to effectively obliterate the earlier scalloping, estimated at a minimum depth of 10 mm of wall rock. A good example is seen in the Clearwater River passage, where scalloping is present at river level, but absent approximately 10–15 m higher (Fig. 2). Counterintuitively the original vadose scallops are sometimes locally preserved where thin films of saturated water run down the walls, with the scalloping being absent on adjacent passage walls. This suggests that the thin film of water prevents any secondary dissolution, preserving the scallops.

In many higher-level (older) passages where the small fluvial scallops are absent, we observed larger scallop-type forms (termed megascallops) often exceeding 1 m in length (Fig. 3; Plan et al., 2012). Classically, these would be attributed to slow flow under phreatic conditions; however, they are too large to be easily explained by this process. They also occur in passages with vadose notches formed by sediment alluviation (Farrant et al., 1995; Farrant and Smart, 2011). This contradictory juxtaposition of vadose and supposed phreatic features in the same passage suggests that the megascallops are formed not by water flow but other processes. Other dissolutional speleogens within the caves are suggestive of features formed by warm air sublimation and ablation on ice surfaces, such as glaciers or ice caves (Bushuk et al., 2019). These ‘aero-speleogens’ include streamlined fluting of the passage walls, with a morphology suggestive of dissolution by a low viscosity fluid. Calcite veins and fossils often stand proud as the surrounding limestone has been dissolved. The resulting small protrusions on the bedrock walls, as well as small stalactites often have a distinctive bedrock ridge in the airflow lee of the protrusion (Audra et al., 2016). In some cases, a horseshoe shaped ‘bow-wave’ dissolutional niche is formed on one side of the projection, facing the direction of the dominant air flow. These features also occur on the dominant airflow side of stalactites hanging from the ceiling, strongly suggesting a post-speleogenetic, sub-aerial origin (Fig. 3).

Another distinctive feature of the Mulu caves is the widespread rounding and smoothing of the bedrock walls and breakdown collapses, which have been observed previously (Audra et al., 2016). These walls and boulders have clearly been rounded by dissolution subsequent to their collapse but lack evidence of fluvial erosion. Many bedrock projections have been similarly subjected to corrosion, producing characteristic bedrock fins and corroded *hoodoo* type features (Fig. 4; Audra et al., 2016). These features have previously been thought to be due to paragenetic dissolution beneath a sediment fill. While paragenesis has undoubtedly occurred (Smart et al., 1985), these projections are also found above the level of the sediment fill. They are distinct from the classic paragenetic pendants and anastomosing rising half tubes (Farrant

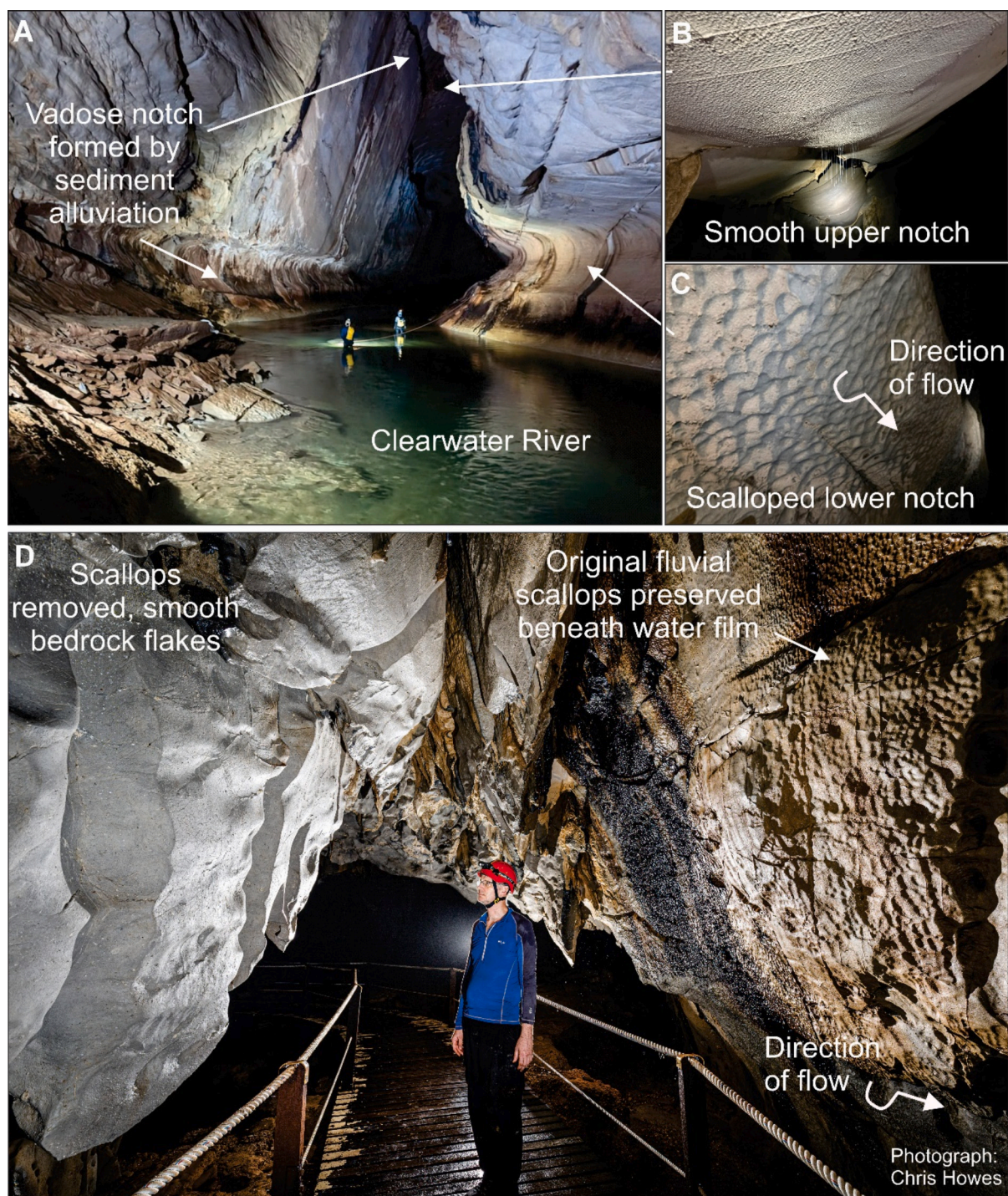


Fig. 2. A. The Clearwater River passage; conspicuous and abundant fluvial vadose scalloping is evident in the lower notch, but absent or very faint in the upper notch and higher passages due to secondary dissolution. B. Detail of smooth upper notch, 30 m above river level. C. Scalloped lower notch, 5 m above river level indicative of fast vadose flow. D. Fast Lane show cave path, Lagang's Cave. The smooth bedrock fins on the right has undergone secondary dissolution while the left side, washed by a film of water preserves abundant vadose scallops due to removal of ammonia and associated wall rock microbial communities.

and Smart, 2011) seen throughout the Mulu caves where the sediment fill has been removed. Some passages contain localised areas of what appears to be highly corroded bedrock, creating *boneyard*- or *sponge-work*-type passage morphology (Fig. 4). This morphology is characterised by large pendants, sculpted rock fins, eroded rock ribs and deeply corroded, heavily rounded bedrock forms (Audra et al., 2016). These features can be seen throughout the cave system, notably in the lower level of Racer Cave, in the 'Snowslopes' area of the Clearwater Cave, and in Stone Horse Cave. Such corroded bedrock features are more usually

associated with hypogene caves, which form through ascending sulfidic or thermal water (DuChene et al., 2017); however, as with the megascallops, in Mulu such features are associated with epigenic features, such as vadose notches or above sediment fills. These corroded features also lack other evidence for a hypogenic origin, such as cupolas or other features characteristic of the morphological suite of rising flow (Klimchouk, 2009).

In many tropical caves, small pits etched into the bedrock or on boulders are common (Fig. 5). These pits, termed 'guano holes' by

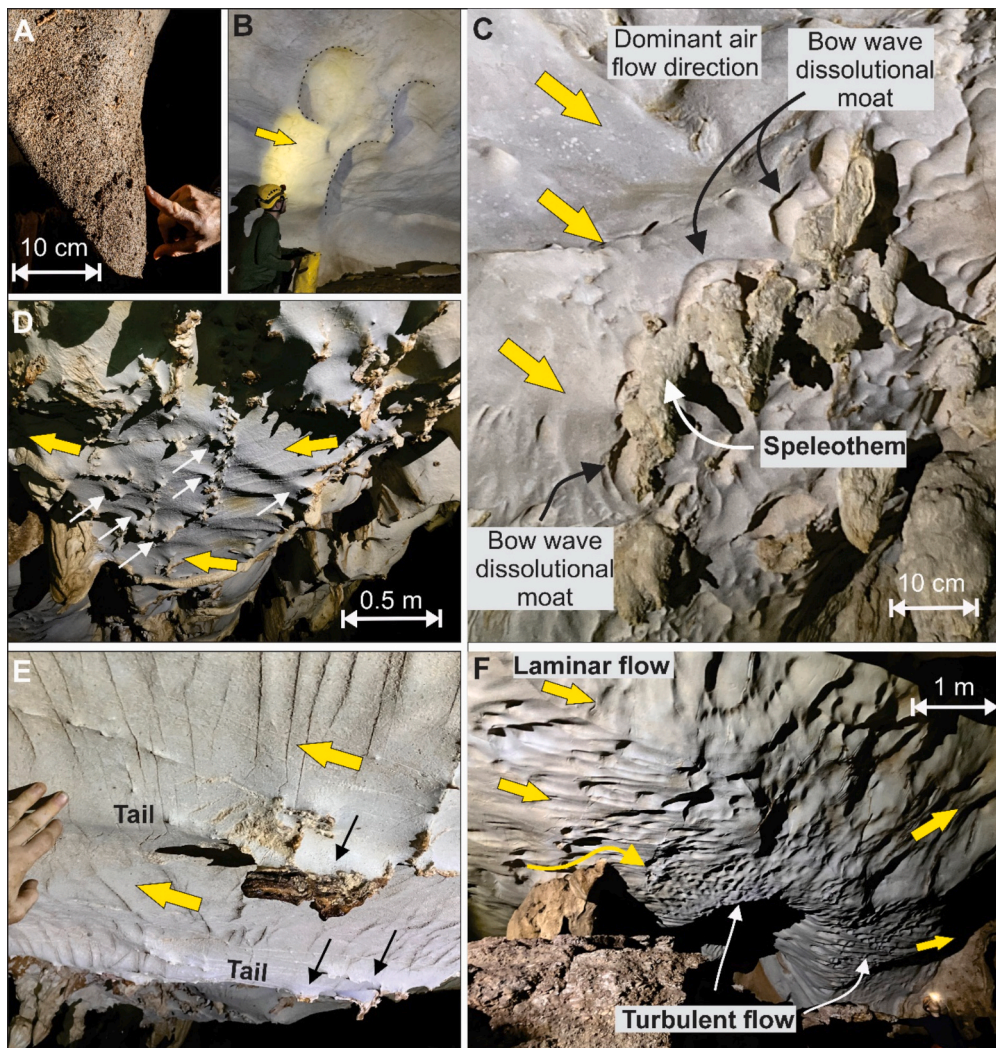


Fig. 3. Subaerial speleogens with direction of dominant wind flow arrowed in yellow. A. Corroded pendants with fossils and other grains etched out, Lagang's Cave (Photograph Chris Howes). B. Proposed megascallop features 1–2 m across, Racer Cave, figure for scale. C. Streamlined fluting around a speleothem, forming a horseshoe shaped 'bow-wave' dissolutional moat, Stone Horse Cave. D. Bedrock fluting around speleothems and calcite veins with a distinctive ridge of bedrock (arrowed) in the lee of the dominant airflow (Stone Horse Cave). E. Ridges of bedrock with 'tail' left by approximately 5–10 cm of subaerial dissolution around small speleothems (arrowed), with thin calcite veins also etched out, Stone Horse Cave. F. Subaerial laminar flow fluting and change to turbulent flow type features in a 15 m wide, 10 m high passage (Stone Horse Cave).

Calaforra et al. (2019, 2022) and 'guano pots' by Audra et al. (2016, 2019), are typically a few centimetres deep and wide, but locally up to 1–2 m deep. They often contain guano and are lined with a phosphatic crust. They can locally be so numerous as to create areas of pitted and honeycombed rock, especially beneath large drips. A related biogenic feature are the small dissolutional niches observed on passage walls above swiftlet nesting or roosting sites. These typically have an inverted conical form, flaring upwards from a small pit or ledge. The pits are commonly infilled with small amounts of guano and are often lined with a phosphatic crust.

In addition to corrosion features and guano alteration crusts, many rock surfaces throughout the cave have developed a distinctive weathering rind (or corrosion residue) typically a few mm to 1–2 cm thick (Fig. 6). This rind comprises a carbonate paste that can be easily removed with a fingernail. It appears to form where changes in air flow following dissolution leads to cyclic evaporation creating an amorphous crust of calcium carbonate or from partial disaggregation of the porous carbonate rock by selective dissolution of more soluble grains and cements. We examined this paste using fluorescence microscopy and noted a high level of microbial cells present. Of the six samples examined, the

number of microbial cells ranged from 7.3×10^7 to 6.0×10^{11} cells/g dry material; this is significantly higher than cell numbers seen on corrosion residues seen on other non-tropical cave surfaces which are typically low, between 10^4 and 10^5 cells/g (Busquets et al., 2014; Barton et al., 2006; Barton and Jurado, 2007; Farnleitner et al., 2005; Newton et al., 2011; Smith et al., 2012) suggesting a large amount of microbial activity was occurring in these pastes. The rind sometimes sloughs off, but on wet walls or ceilings a distinctive 'cockling' texture can be observed. In other areas, the soft, unconsolidated rind is washed down the walls by condensation or percolation waters, forming a thicker crust with a cottage cheese type texture (Fig. 6) that is distinct from the more common moonmilk residues. Locally this paste can form globules of dried, remobilised calcium carbonate at the base of pendants or rock protrusions (Fig. 6).

Throughout the Mulu Caves, corroded speleothems are common with dissolution so intense that stalagmites several metres across have been eroded to the core (Fig. 7). Similar speleothem corrosion has been noted from other guano-rich caves (Audra et al., 2016; Dandurand et al., 2019), but in the Mulu caves they are not exclusively juxtaposed to major bat roosts but throughout the caves. In areas of intense secondary

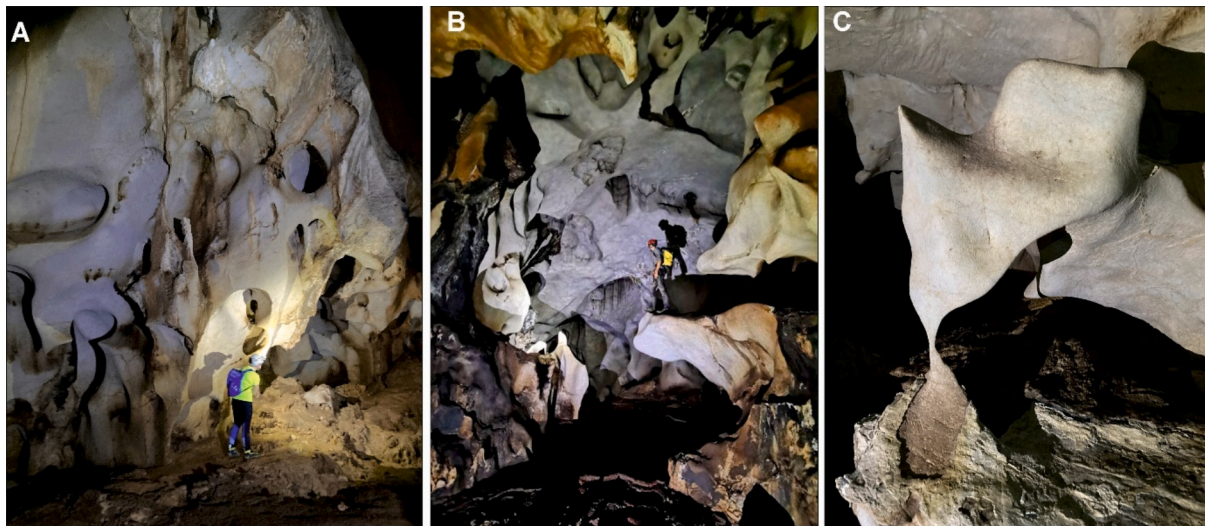


Fig. 4. Examples of boneyard- or spongework-type passage morphology. A Racer Cave (lower level). B. Snowslopes in Clearwater Cave. C. Bedrock hoodoo in Stone Horse Cave (approximately 1 m high).

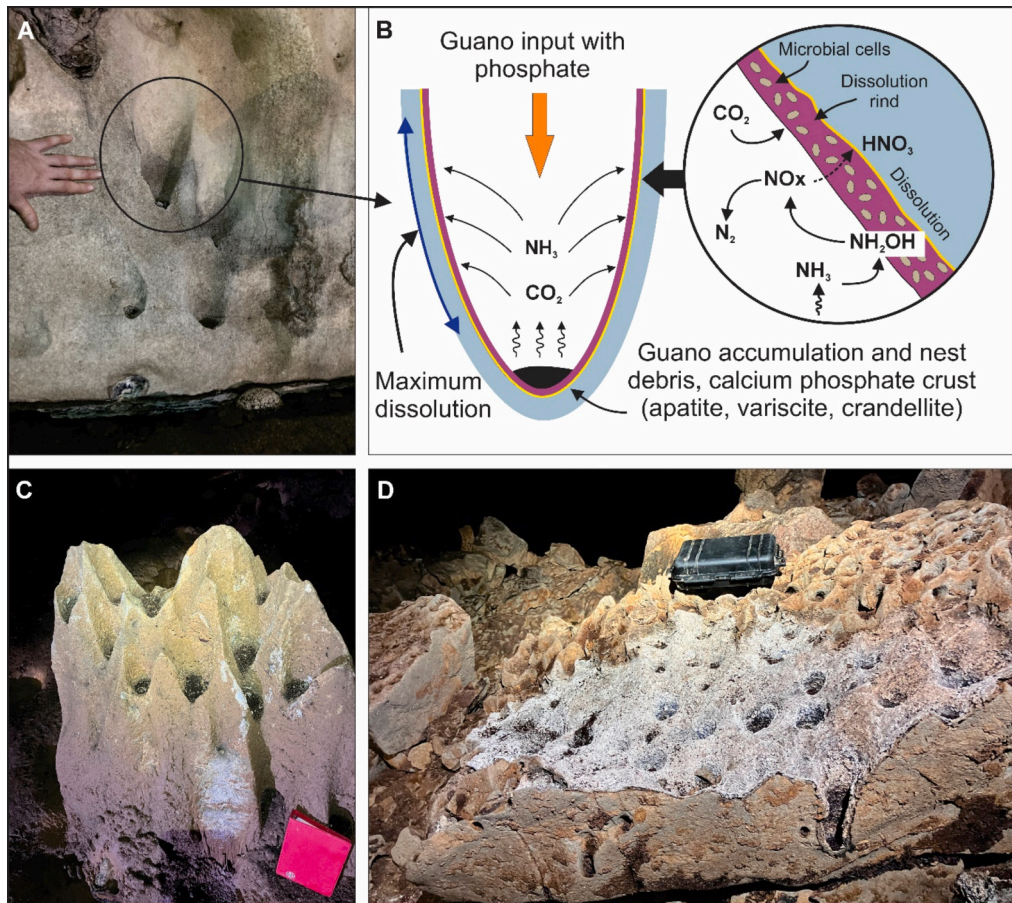


Fig. 5. Guano holes and dissolutional niches. A. Passage wall in Stone Horse Cave with upwards flared conical dissolutional niches, sometimes used by swiftlets as nesting sites. B. Niche formation mechanism with dissolution due to ammonia nitrification from swiftlet guano; most dissolution occurs where ammonia is absorbed onto the niche walls, with phosphate in the guano reacting to form hydroxyapatite crusts. C. Example of guano holes on boulder, Racer Cave. D. Guano holes with hydroxyapatite crust, Lagang’s Cave.

dissolution, corroded stalagmites have been observed atop a bedrock stump (Fig. 7). Examples can be seen in Racer Cave, Clearwater Cave (St. Lawrence, 2015) and many other locations. The implication is that the stalagmite has protected the underlying bedrock from secondary

dissolution in much the same way as a glacial erratic sometimes protects the underlying limestone from dissolution, creating a pedestal (Goldie, 2005).

Collectively, the geomorphology of the Mulu caves suggests that

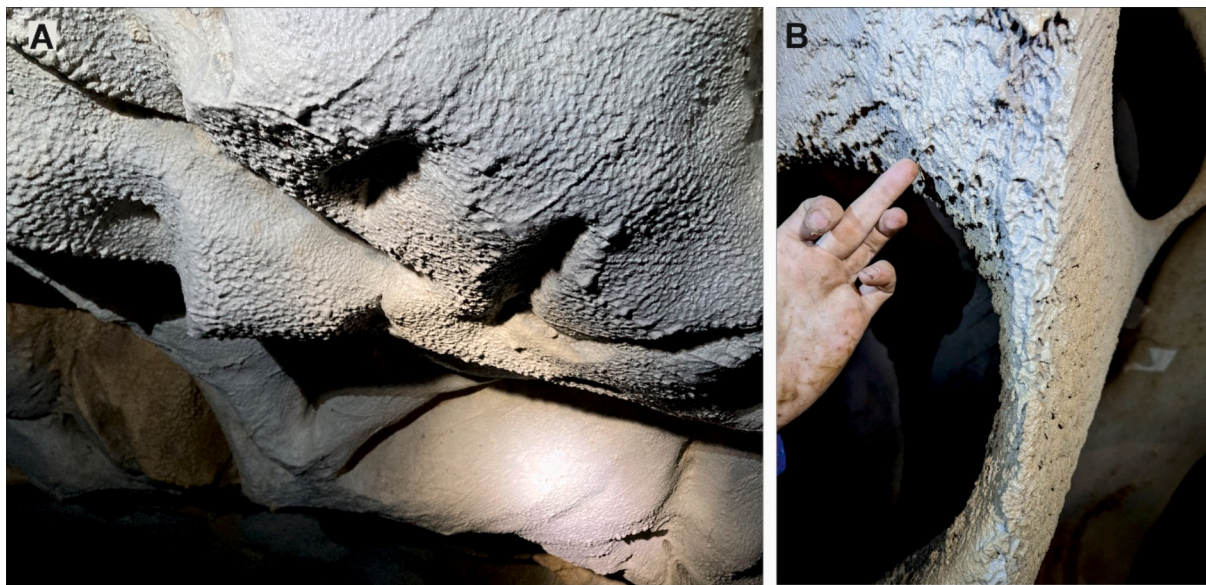


Fig. 6. Carbonate weathering rind and ‘cockling’ textures preserved on the passage walls and roof of many cave passages in Mulu. A. Paste on the wall and ceiling of Fast Lane, Lagang’s Cave. B. Remobilised paste on spongework, Racer Cave.



Fig. 7. Corroded speleothems from Racer Cave. A. Stalagmite boss on the wall corroded to bedrock revealing the growth banding. B. A corroded pinnacle, the upper 2–2.5 m is partially dissolved speleothem, the lower part limestone bedrock.

post-abandonment enlargement through subaerial corrosion is widespread throughout caves. It is not limited to areas in close proximity to animal roosts and rules out an exclusive role for localised biogenic condensation corrosion. While local biogenic effects explain some small-scale features, such as the bell holes and apse flutes seen in Deer Cave, the observed dissolution morphologies throughout the remainder of the caves (Fig. 8) must be caused by another process. Condensation corrosion is a possible mechanism, which occurs when air is cooled below its dew-point temperature, condensing on surfaces and leading to dissolution; however, condensation is negligible in cave interiors that have stable temperatures at or close to the mean annual exterior temperatures. Modelling further suggests that condensation corrosion is likely to drop off rapidly away from cave entrances, typically within a distance of $5x$, where x represents the entrance width (Wigley and Brown, 1971). In

the Mulu caves, the strong flows of both air and water, coupled with diurnal changes in air flow direction can allow condensation and evaporation to occur significant distances from the entrance, more than the distances suggested by Wigley and Brown (1971). However, some areas in the Mulu caves where extensive condensation has been observed do not exhibit significant corrosion and vice versa. Likewise, caves with significant condensation corrosion, such as Lechuguilla Cave do not display the aggressive erosion of surfaces seen in the Mulu caves. We therefore undertook an extensive physical and geochemical assessment of the caves to identify the factors that could be causing the extensive secondary enlargement observed.

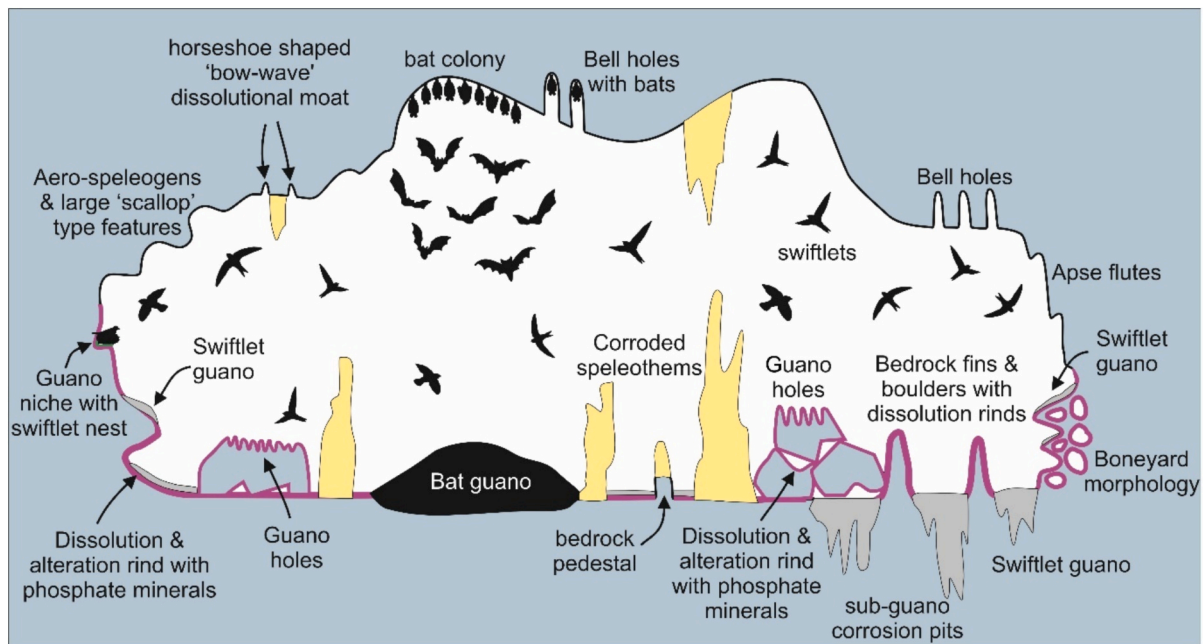


Fig. 8. Summary of the biogenic dissolution features observed in the Mulu caves.

4. Methods

To investigate the impact of bird and bat populations on the geomorphology of the cave systems, and to identify the possible mechanism for continued sub-aerial dissolution, we undertook geochemical analyses of guano, dissolution residues and cave waters. Physiochemical measurements including pH and water content of both bat and swiftlet guano were measured, and the mineralogy of the guano-rock interface examined to explore the chemistry of each guano pile. In situ measurements of water chemistry were analysed using various methods. Temperature, pH, and conductivity were taken using standard field pH and conductivity meters. Water quality test strips were used to provide a quick, albeit relatively imprecise, indication of the chemical composition of the drip-waters. The advantage of these is that they can be done in the cave with instant results and deployed quickly at multiple locations. The strips used test for pH, conductivity, alkalinity, nitrate, nitrite, ammonia, sulphate, chlorine (free and total) and total hardness. This was backed up by in-situ analysis using a DR1900 Portable Spectrophotometer and a SL1000 Portable Parallel Analyzer. In addition, water samples were collected from the caves and analysed in the lab by ion chromatography for the anions and trace and major elements by ICP-MS.

Condensation water was also collected from a Perspex screen on the show-cave path in Cave of the Winds and from ice bottles suspended within the caves. In addition to the drip waters, water samples were collected from within swiftlet guano pile in Easter Cave, a bat guano pile in Deer Cave, and from the bedrock alteration rind on the passage wall in Racer Cave. A portable ammonia Gas Detector (GD200-NH3) was used to sample the air within the caves. The in-situ water testing using the DR1900 Portable Spectrophotometer and the SL1000 Portable Parallel Analyzer showed similar results.

To assess whether the condensation and percolation drips were sufficiently aggressive towards cave wall-rock and stalagmite calcite to generate the dissolutional forms observed, we tested the chemical aggressiveness of the waters. A very simple, direct and effective technique is to measure the Stenner Aggressiveness (Stenner, 1969). Two aliquots of the water in question are sampled. To one sample is added an excess amount of pure calcium carbonate, the other is left as collected. After being left for a short period of time to equilibrate, the two samples are titrated for total hardness; the difference between the two

measurements indicate super- or under-saturation. If after adding CaCO_3 the hardness increases, the water was aggressive and had further dissolution capacity. On the contrary, a supersaturated sample would be nucleated by the added calcite and total hardness would drop (Lauritzen, 1981). Electrical conductance can be used as a hardness proxy (the relationship between hardness and electrical conductance is linear). Condensation water, percolation droplets, and drips from straw stalactites were collected with a polyethene pipette in the cave and transferred to 50 ml sample vials. Fresh condensation water was collected on plastic bottles containing ice and placed in the cave sites. To one aliquot was added an excess CaCO_3 paste with a spatula and closed. In situ conductivity and pH were measured on site and were measured again later.

5. Geochemical evidence for post-abandonment biogenic dissolution

5.1. Guano geochemistry

The secondary dissolution features observed in the Mulu caves occur away from significant bat populations, suggesting that differences in the chemistry of bird and bat guano may be a contributing factor. Physiological differences occur in how bats and birds excrete nitrogenous waste: bats, as mammals, excrete nitrogenous waste as urine whereas birds store nitrogenous waste and uric acid in the cloaca, which is excreted during defecation. Both contain high levels of phosphates. To distinguish the chemistries between bird and bat guano, we sampled two caves: Deer Cave, which supports a large population of insectivorous wrinkle-lipped bats; and Easter Cave, which supports a significant population of insectivorous birds, which fly deep into Easter Cave from various entrances. At the sample site in Easter Cave, the bird guano spreads across the whole passage, with significant evidence of biogenic weathering. Several guano piles were investigated, and the average results for these analyses are presented.

There was a distinctive difference in the structure between the different types of guano. The bat guano accumulates in large piles on surfaces, which in places are almost 1 m deep. The bird guano piles are flat, having dissolved the surface below up to a maximum depth of 20 cm. In Easter Cave, (and in many other Mulu caves), conical dissolution

pits typically a few cm wide, but locally 0.5–1 m deep are often seen on rock surfaces, especially along bird flight paths and roosting sites. These contain small pockets of guano (the ‘guano holes’ of Calaforra et al., 2019). On flat or gently sloping surfaces, these can combine to form a highly irregular ‘eggbox’ type micro-topography (Fig. 5).

A comparison of bat and bird guano piles indicated that the bird guano was wetter: 59 % wet weight at the surface and 66 % wet weight at the guano-rock interface (at 15 cm), compared to bat guano with 45 % wet weight at the surface and 33 % wet weight at the rock-guano interface (at 40 cm). Of note is that the bat guano is comparatively low-density granular material, composed largely of chitinous insect wing carapaces, whereas the bird guano was wetter, often more of a granular slurry. The bird guano was also more acidic, with a pH of 1.9 at the surface and pH 2.7 at the rock-guano interface, which the bat guano had a pH of 3.6 at the surface and pH 3.4 at the rock-guano interface. Interestingly, when wet litmus paper was held directly above the surface of the bird guano pile, it indicated alkali conditions (~pH 8.0), despite the acidic conditions of the guano. No such observation was made above the bat guano. To determine whether this phenomenon was unique to the sample site in Easter Cave, we repeated this test on numerous guano piles throughout the Mulu caves – consistently we only saw the pH 8.0 measurement above bird guano piles.

The amount of nitrogen and phosphorous in bird and bat guano is highly variable, depending on the diet of the animal (insects, nectar, nuts/seeds, etc.). We focused on two insectivorous species and compared the N content. While the bat guano contained higher N levels, the amount varied with depth: bat guano was ~8.8 % N at the surface and 2.4 % N at the rock-guano interface, while the bird guano was ~5.3 % N guano at the surface and ~2.6 % N at the rock-guano interface. As a preliminary analysis of the fate of the N in these guanos, we examined the bulk $\delta^{15}\text{N}$ values of both the surface and rock-guano interface. In bat guano, the surface of the guano was $\delta^{15}\text{N}$ 4.6 ‰, with the rock-guano contact $\delta^{15}\text{N}$ 16.8 ‰, which contrasted with the bird guano: $\delta^{15}\text{N}$ 5.3 ‰ at the surface and $\delta^{15}\text{N}$ 3.4 ‰ at the rock-guano interface. These inverted isotopic values may reflect the different mechanisms microorganisms mineralize urea and uric acid to ammonia: urea is broken down by urease, which hydrolyses urea into ammonia and CO_2 , using water as a source of the attacking hydroxyl group in an oxygen-independent reaction; uricase facilitates the breakdown of uric acid into allantoin, with oxygen serving as an electron acceptor for catalysis. As a result, uric acid breakdown is confined to aerobic zones within the guano pile. In the bat guano pile, mineralization of urea can occur throughout the pile, while in the bird guano the initial breakdown of uric acid to urea can only occur near the surface, under aerobic conditions, while urea breakdown can continue through the full depth of the guano.

The nitrogen cycle in organic deposits can be complex, and changes in N isotopic composition are not clearly defined, although some work has been carried out on composting animal waste and urine in soils. These data indicate that $\delta^{15}\text{N}$ increases dramatically through the volatilization of ammonia, with enrichments $\delta^{15}\text{N} > 15$ ‰, while the mineralization of organic N can also increase $\delta^{15}\text{N}$ enrichment > 10 ‰ (Kim et al., 2008; Frank et al., 2004; Bokhorst et al., 2019). We believe our data demonstrates that urea breakdown to ammonia is occurring throughout the bat guano pile, with either older guano deposits or additional organic N mineralization occurring at the guano-rock interface. In the case of the bird guano, the $\delta^{15}\text{N}$ values suggest that majority of ammonia loss is occurring at the surface, where uric acid is presumably being broken down. It is difficult to determine the chemistries dominating at the bird guano-rock interface, although sedimentary mineralization of organic N can increase the relative concentrations of $^{14}\text{NO}_2^-$ and $^{14}\text{NO}_3^-$, which may explain the reduced ^{15}N enrichment (Sebilo et al., 2019). Nonetheless, without a better understanding of the ^{15}N values of fresh guano and a detailed understanding of the isotopic values of the different N species in the various steps of urea/uric acid breakdown and guano composition, such findings remain preliminary. More work is being carried out to further clarify the fate of N in these

systems using isotopic data.

To resolve what chemistries may be present in the guano, we examined the minerals at the rock-guano interface. At the bottom of both the bat and bird guano a white paste was consistently found. In the bat guano this was identified as hydroxyapatite $[\text{Ca}_{10}(\text{PO}_4)_6(\text{OH})_2]$, variscite $(\text{AlPO}_4 \cdot 2\text{H}_2\text{O})$, and brushite $(\text{CaHPO}_4 \cdot 2\text{H}_2\text{O})$, all of which are indicative of phosphoric acid attack of the limestone. In the bird guano pile, only hydroxyapatite was detected. Where the top of the bat guano contacted the host rock, a crust of crandallite $[\text{CaAl}_3(\text{PO}_4)(\text{PO}_3\text{OH})(\text{OH})_6]$ and calcium aluminium oxide was formed. Both are rich in aluminium, probably derived from the leaching of aluminium-rich fluvial clays and decomposed sandstone and siltstone cobbles washed in by the formative river from the adjacent Mulu Formation; however, where the surface of the bird guano come into contact with the limestone rock piles, the mineralogy was very different. At the top of the pile, we identified tetramethylammonium carbonate $[(\text{CH}_3\text{CH}_2)_4\text{N}(\text{HCO}_3)]$, ammonium calcium phosphate $(\text{CaH}_4\text{NO}_4\text{P})$, and calcium hydride nitride (Ca_2NH) , indicative of significant amounts of ammonia interacting with the limestone.

5.2. Water chemistry

A second approach focussed on water-chemistry. Several distinct water sources are present in the caves; autogenic drip-waters from stalactites and flowstones, condensation droplets on the cave walls, percolation drips derived from matrix flow within the porous limestone bedrock, vadose autogenic stream inlets, and allogenic cave streams. These are characterised by different in-cave residence times. The stalagmite drip water and vadose stream inlets are relatively rapid, flowing water with short residence times in the cave air typically measured in seconds to minutes. The condensation drops on the cave walls have potentially long residence times as the drips can sit on the wall for hours to days depending on ambient conditions. Similarly, percolation drops can be present from minutes to hours depending on matrix flow rates.

A range of different water samples were obtained from multiple sites in six caves: Racer Cave (lower level), Lagang’s Cave (Fast Lane), Stone Horse Cave, Deer Cave, Easter Cave and Cave of the Winds with some additional samples from Lady Cave. Condensation water from suspended ice bottles was also collected, which reflects the composition of water vapour within the cave that has not interacted with the cave walls. As a control, samples of rain, river and spring waters were collected. The springs sampled included the main Clearwater River resurgence, the river emerging water from Cave of the Winds, and a spring near the Melinau Paku river on the tourist path to Deer Cave.

The analysis of the water samples suggests significant chemical differences between the different sources of water. The short residence time drip waters from stalagmites and vadose inlets show the least variation, with typical pH values around 8–8.5 indicating saturation with respect to calcium carbonate. These samples typically contained little or no nitrate, nitrite, sulphate, potassium or chlorine (Fig. 9), and low levels of other trace elements and metals. A few had slightly elevated levels of ammonia (0.25–1 ppm). By contrast, the long-residence time waters, particularly the condensation and percolation drips on cave walls had significantly elevated levels of nitrate (Table 1), often beyond the limit of even the high-range testing strip (500 mg l^{-1}). Subsequent laboratory analysis proved very high values sometimes in excess of 6000 mg l^{-1} . For comparison, the European drinking water standard for nitrate is 50 mg l^{-1} . These drops also had elevated levels of the alkaline-earth metals (potassium, magnesium, barium and strontium), as well as sulphate, along with elevated levels of silica (Table 1) and a wide variability in pH and conductivity. Water samples from rainwater and springs were very low, with the highest levels of nitrate (0.7 mg l^{-1}) and phosphorous (0.6 mg l^{-1}) found in samples from the river just downstream from Clearwater Cave resurgence. The ice bottle condensate samples typically had a lower pH (6.7–6.9) than the cave wall samples. As was expected, the total hardness was lowest in the ice

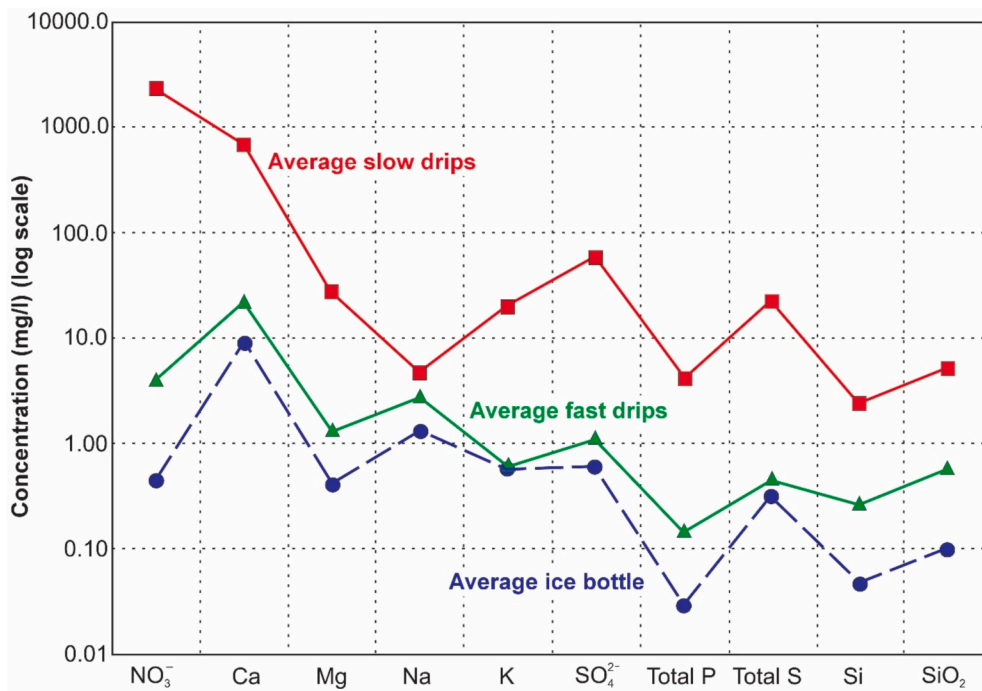


Fig. 9. Concentration of major elements in drip waters from the Mulu Caves. Slow drips with long residence times (percolation and condensation drips) have significantly elevated levels of nitrate derived from ammonia nitrification compared to fast drips from speleothems and vadose inlets. They also have elevated levels of Ca and Mg from dissolution of the limestone bedrock and other elements from airborne dust and guano residues. The ice bottle concentrations reflect the composition of water vapour in the cave air.

Table 1

Geochemistry of various types of drip water. Long residence drip waters shaded (condensation and percolation waters). Nitrate levels highlighted, ranging from very low (0–2 mg l⁻¹), low (2–20 mg l⁻¹), moderate (20–200 mg l⁻¹), high (200–1000 mg l⁻¹) and very high (1000–8000 mg l⁻¹).

Sample	Water Type	Cave	Nitrate levels	pH	NO ₃ ⁻		Ca	Mg	Na	K	SO ₄ ²⁻	Total P	Total S	Si	SO ₂	Ba	Sr	Mn	Al	Ti	V	Cr	Co	Ni	Cu	Zn
					mg l ⁻¹	mg l ⁻¹																				
30509-0001	Condensation drips on wall	Racer Cave	Very High	7.14	7726	<0.25	2149	36.8	0.9	0.20	70.9	<0.02	26.6	5.21	11.1	18.7	3904	5.3	1.0	0.16	11.5	1.41	0.069	0.70	1.47	4.7
30509-0002	Fast Drip (speleothem)	Racer Cave	Very Low	8.46	0.930	<0.05	23.4	0.337	<0.4	<0.04	<0.5	<0.02	0.12	0.338	0.723	0.32	24.2	0.6	1.6	<0.06	0.48	0.44	<0.006	<0.04	0.10	2.8
30509-0003	Percolation drips on passage roof	Lagang's Cave (Fast Lane)	High	n/a	265	<0.05	84.6	5.31	1.7	1.26	1.87	<0.02	1.00	0.607	1.30	1.35	85.3	0.2	0.9	<0.06	4.34	1.26	<0.006	0.05	0.35	0.3
30509-0004	Fast Drip (speleothem)	Lagang's Cave (Fast Lane)	Low	8.25	1.13	<0.05	20.1	0.732	<0.4	0.19	<0.5	<0.02	0.14	0.113	0.242	91.4	17.9	0.2	1.8	<0.06	0.84	0.52	<0.006	<0.04	0.18	13.2
30509-0005	Percolation (Iaguano)	Lagang's Cave (Fast Lane)	Very High	n/a	6194	<0.05	1850	53.7	33.1	10.2	221	27.8	79.4	3.58	7.66	25.8	1388	5800	<0.6	0.93	17.2	0.71	0.899	15.1	68.2	1890
30509-0006	Fast Drip (speleothem drip pool)	Lagang's Cave (Fast Lane)	Low	n/a	11.1	<0.05	25.8	1.43	<0.4	0.41	<0.5	<0.02	0.26	0.477	1.02	1.93	25.6	0.3	2.2	<0.06	1.19	0.95	<0.006	0.06	0.29	1.0
30509-0007	Condensation drips on wall	Lagang's Cave (Fast Lane)	Very High	7.84	1943	<0.05	609	31.1	0.8	1.07	83.2	<0.02	30.2	1.78	3.81	10.0	500	<0.2	1.5	0.08	2.21	1.37	0.074	0.27	2.14	3.1
30509-0008	Fast drip (vadose inlet)	Lagang's Cave (Fast Lane)	Very Low	n/a	1.55	<0.05	20.2	0.659	0.4	0.30	<0.5	<0.02	0.13	0.134	0.287	31.3	13.4	<0.2	2.4	<0.06	0.96	0.50	0.007	0.05	0.57	2.6
30509-0009	Moderate drip (vadose inlet)	Lagang's Cave (Fast Lane)	Low	8.47	2.06	<0.05	18.7	0.700	<0.4	0.08	<0.5	<0.02	0.11	0.167	0.357	0.57	12.8	<0.2	2.1	<0.06	1.07	0.89	<0.006	0.06	0.61	0.9
30509-0010	Condensation drips on wall	Stone Horse Cave	High	6.80	276	<0.05	88.6	13.1	0.4	0.86	10.6	<0.02	4.75	0.570	1.22	11.4	50.7	<0.2	1.3	<0.06	0.80	0.22	0.017	0.07	0.55	1.1
30509-0011	Fast drip (speleothem)	Stone Horse Cave	Very Low	8.17	0.848	<0.05	26.3	1.79	<0.4	<0.04	<0.5	<0.02	0.15	0.144	0.308	0.21	11.4	<0.2	1.3	<0.06	0.37	0.28	<0.006	0.05	0.20	0.3
30509-0012	Condensation drips on wall	Stone Horse Cave	Very High	n/a	5997	0.079	1682	112	14.3	121	277	6.33	101	5.41	11.6	78.9	843	81.6	<0.6	0.28	0.22	0.17	0.224	0.88	2.43	22.6
30509-0013	Moderate drip (speleothem)	Stone Horse Cave	Low	8.59	9.61	<0.05	3.2	3.76	37.1	0.08	<0.5	<0.02	0.18	0.185	0.396	0.32	3.8	<0.2	7.1	<0.06	1.24	0.70	<0.006	<0.04	0.22	0.6
30509-0014	Condensation drips on perspex screen	Cave of the Winds	Moderate	n/a	28.6	0.096	7.9	0.184	8.0	5.59	6.82	<0.02	0.52	<0.042	<0.09	15.3	6.1	20.5	7.8	0.11	0.08	0.96	0.399	8.36	13.4	6591
30509-0015	Condensation drips on wall	Cave of the Winds	High	n/a	823	0.284	275	9.28	6.5	38.8	42.1	5.02	16.4	0.960	2.05	150	370	3.2	2.5	0.24	0.48	0.16	0.111	1.25	2.71	131
30509-0016	Fast drip (speleothem)	Cave of the Winds	Very Low	7.95	1.25	<0.05	24.8	0.449	0.7	0.66	<0.5	<0.02	0.16	<0.042	<0.09	8.37	19.8	5.8	1.7	<0.06	0.35	0.12	0.047	0.68	5.50	641
30509-0017	Condensation drips on wall	Cave of the Winds	High	8.25	244	<0.05	19.6	15.7	<0.4	0.12	40.2	<0.02	15.2	1.08	2.31	4.43	395	<0.2	1.6	0.08	6.41	0.19	0.016	1.74	0.50	2.2
30509-0018	Fast Drip (speleothem)	Cave of the Winds	Very Low	8.47	0.764	<0.05	19.1	0.458	<0.4	0.20	<0.5	<0.02	0.11	0.068	0.145	8.80	24.7	<0.2	3.2	<0.06	1.29	0.24	0.011	0.20	0.75	10.5
30509-0019	Fast Drip (speleothem)	Stone Horse Cave	Low	8.50	18.7	<0.05	28.2	1.15	<0.4	2.94	9.01	<0.02	0.63	0.352	0.753	0.81	15.6	<0.2	1.5	<0.06	0.47	0.26	<0.006	0.14	0.34	0.4
30509-0020	Condensation drips on wall	Stone Horse Cave	Very High	n/a	4096	<0.05	1216	52.7	7.3	63.4	123	16.3	47.0	7.38	15.8	38.6	605	285	1.3	0.57	0.35	0.22	0.229	10.2	4.28	402
30509-0021	Water in guano pocket	Stone Horse Cave	Moderate	8.47	67.5	<0.05	30.2	1.79	<0.4	1.35	1.22	<0.02	0.67	0.516	1.10	0.58	19.7	<0.2	2.5	<0.06	0.52	0.05	<0.006	<0.04	0.45	1.0
30509-0022	Spring	Malinau Paku spring	Low	7.75	2.01	<0.05	20.9	1.00	<0.4	0.15	<0.5	<0.02	0.17	1.16	2.48	1.53	16.0	0.5	2.2	<0.06	0.40	0.09	<0.006	0.06	0.27	1.8
30509-0023	Condensation drips on wall	Lagang's Cave (Fast Lane)	Very High	7.55	1642	<0.05	511	32.6	<0.4	0.43	40.5	<0.02	15.8	0.313	0.670	6.48	45.7	0.5	2.2	0.22	1.10	0.83	0.033	0.69	4.80	34.8
30509-0024	Percolation drips on passage roof	Lagang's Cave (Fast Lane)	High	8.15	228	<0.05	80.8	5.46	1.0	0.91	1.31	<0.02	0.80	0.856	1.40	1.29	89.9	<0.2	1.7	<0.06	5.90	0.89	0.114	0.15	0.13	2.9
30509-0025	Rainfall	Rainfall	Very Low	6.86	0.311	<0.05	1.2	0.025	<0.4	0.20	<0.5	<0.02	0.05	0.103	0.220	1.22	7.8	5.1	1.1	<0.06	0.07	<0.004	0.08	0.13	0.45	1.0
30308-0001	Icebottle	Racer Cave	Very Low	6.8	0.327	0.894	4.7	0.289	1.4	0.38	0.487	0.096	0.26	<0.042	<0.090	3.3	17.7	11.3	<2	<0.5	0.17	0.12	0.042	0.22	1.46	24.5
30308-0002	Moderate drip (vadose inlet)	Cave of the Winds	Low	7.9	13.7	0.007	17.4	0.780	1.1	0.18	0.453	<0.005	0.22	1.01	2.16	3.0	36.0	0.5	<2	<0.5	0.63	0.25	0.012	0.13	2.30	0.5
30308-0003	Icebottle	Lagang's Cave (Fast Lane)	Very Low	6.9	<0.03	<0.005	8.4	0.415	1.6	1.45	0.450	0.034	0.38	<0.042	<0.090	14.2	21.0	378	6	<0.5	0.20	0.23	1.29	15.2	12.3	125
30308-0004	Icebottle	Stone Horse Cave	Very Low	6.7	0.455	<0.005	6.5	0.278	1.6	0.37	0.340	<0.005	0.17	<0.042	<0.090	4.0	16.9	8.8	<2	<0.5	0.08	0.22	0.059	0.96	5.32	8.2
30308-0005	Icebottle	Lagang's Cave (Fast Lane)	Very Low	n/a	1.04	<0.005	19.4	0.853	0.6	0.07	0.407	<0.005	0.20	0.062	0.133	1.7	30.6	0.4	<2	<0.5	0.90	0.62	<0.006	<0.05	0.76	0.7
30308-0009	Condensation drips on wall	Lagang's Cave (Fast Lane)	High	8.1	242	<0.005	87.5	6.40	2.1	1.80	3.04	0.086	1.15	0.712	1.52	4.1	121	1.3	<2	<0.5	4.85	0.13	0.008	0.43	61.9	6.3
30308-0010	Fast Drip (speleothem)	Lagang's Cave (Fast Lane)	Low	7.9	2.18	0.006	19.4	0.877	0.7	0.07	0.626	0.027	0.28	0.097	0.208	1.9	30.6	<0.2	<2	<0.5	0.43	0.21	<0.006	0.05	1.16	1.1
30308-0011	Condensation drips on wall	Lagang's Cave (Fast Lane)	High	7.3	565	0.011	196	12.1	2.3	0.37	11.2	0.016	4.44	1.21	2.59	18.0	289	1.2	<2	<0.5	1.61	0.33	0.028	0.38	5.52	24.9
30308-0012	Fast Drip (speleothem)	Lagang's Cave (Fast Lane)	Very Low	7.9	1.07	<0.005	19.2	0.789	0.6	0.08	0.493	0.010	0.23	0.064	0.137	1.8	38.2	0.6	<2	<0.5	0.80	0.53	0.007	0.07	20.4	2.1
30308-0013	Condensation drips on wall	Lagang's Cave (Fast Lane)	Moderate	7.9	79.7	<0.005	40	4.41	5.5	1.34	4.72	5.99	1.84	0.620	1.33	6.0	80.5	3.3	8	<0.9	8.1	0.67	0.036	0.62	5.85	2.1
30308-0014	Fast Drip (speleothem)	Lagang's Cave (Fast Lane)	Very Low	8.1	1.66	<0.005	22.6	0.931	0.6	0.12	0.628	0.057	0.30	0.048	0.103	3.6	33.9	0.3	2	<0.5	0.82	0.38	0.021	0.13	110	4.8
30308-0015	Fast Drip (dripwater pool)	Lagang's Cave (Fast Lane)	Very Low	8.0	0.156	<0.005	33.0	2.31	1.4	3.41	1.69	2.11	0.98	0.163	0.349	2.1	43.3	2.7	<2	<0.5	0.71	0.17	0.129	0.40	15.7	3.7
30308-0016	Icebottle	Stone Horse Cave	Very Low	6.7	0.378	0.091	6.3	0.239	1.3	0.63	1.28	<0.005	0.53	<0.042	<0.090	4.7	15.6	3.7	3	<0.5	0.10	0.08	0.047	0.42	4.01	12.7
30308-0017	Fast Drip (speleothem)	Racer Cave	Very Low	7.4	0.989	<0.005	28.9	0.574	0.7	0.06	0.646	0.130	0.29	0.366	0.826	2.9	44.2	0.2	<2	<0.5	0.79	0.34	<0.006	<0.05	1.77	0.4
30308-0018	Condensation drips on wall	Racer Cave	Very High	6.9	6245	<0.005	2085	37.9																		

bottle condensate, and much higher in the cave wall and stalactite drip samples. Levels of nitrate and nitrite were very low, and no samples contained any significant chlorine, sulphate or phosphate.

Trace element analysis by ICP-MS showed a similar differentiation between the long residence time drip waters and the rapid throughput waters (Table 1). The slow drips had elevated levels of trace metals compared to that found in the fast drips. High values of copper (up to $130 \mu\text{g l}^{-1}$) and zinc ($6591 \mu\text{g l}^{-1}$) are present, but also elevated amounts of nickel, vanadium, strontium, uranium, selenium and rubidium. Likewise, levels of cadmium, tin, antimony and caesium were also elevated. Levels of the rare earth elements were below the limit of detection in most samples.

It is unlikely that the elevated metal and trace element concentrations seen in the slow drip waters are derived from the limestone bedrock, which is mostly low-Mg calcite. No significant mineral veins or ore deposits are known in the Melinau limestone. Instead, they are likely to be derived from guano deposited within the caves. Wurster et al. (2015) found extremely high concentrations of transition metals in modern and ancient bat guano across southeast Asia relative to the local environment. Copper and zinc levels in the guano profiles they measured are considerably enriched, with copper levels in excess of 7500 mg/kg at the Gangub, Makangit, and Batu Caves, and c. 2300 mg/kg in the Niah and Gomantong caves in Borneo. These elements are bioaccumulated via plants to insects and ingested by feeding bats and swiftlets. These bioaccumulated metals, along with other organic materials (chitin, keratin) are excreted within the cave. While the bat guano tends to be concentrated around bat roosts, swiftlet guano is more widespread. Moreover, the nesting habits of swiftlets on ledges and rock niches facilitates the deposition of guano on the passage walls below nesting sites. Some of this guano is subsequently remobilised by other organisms and water flow. The subsequent microbial degradation of guano leaves behind an enriched residue high in metals and trace elements, which is incorporated into percolation and condensation drip waters. Some of highest levels of metals and trace elements measured in the Mulu caves (sample 30,509-0005, Fast Lane, Lagang's Cave,

Table 1) were from a slow drip fed by water percolating through a guano filled alcove.

5.3. Determination of chemical aggressiveness

The results of the aggressiveness tests (Stenner, 1969) show a clear distinction between condensation waters collected on the ice bottles, which were very aggressive and the cave wall drip samples. Most of the cave drip samples were saturated, but some were significantly under-saturated, indicating that they were actively dissolving the bedrock. Those that were saturated tended to have higher conductivity values, suggesting they had dissolved up the bedrock, increasing their hardness. Fig. 10 shows quite clearly the aggressiveness of fresh condensation water and partial saturation as soon as the water has been in contact with rock surfaces. This demonstrates that the water droplets on the cave walls were sufficiently aggressive to cause dissolution.

6. Dissolution mechanism

The widespread evidence of subaerial dissolution seen in the Mulu caves and the elevated nitrate levels seen in water found on surfaces cannot be easily explained by existing models of fluvial and condensation corrosion. Instead, we propose that microbial oxidation of ammonia derived from guano decomposition occurs on cave passage walls (Fig. 11), driven by the unusually high microbial load seen in the cave wall dissolution residues, generating nitric acid and causing dissolution. This hypothesis is similar to the release of nitric acid by the mineralization of bat guano proposed by Audra et al., 2019, while explaining the stark difference in nitrate levels between the short and long-residence time water sources across the scale of the whole cave. The lack of significant nitrate, nitrite, or ammonia in the measured infiltrating water suggests the nitrate observed in the percolation and condensation drips is not being washed in but is generated locally. Slightly elevated levels of ammonia were detected in some slower drips, or where the drips were sourced from water flowing down a rock face prior to collection,

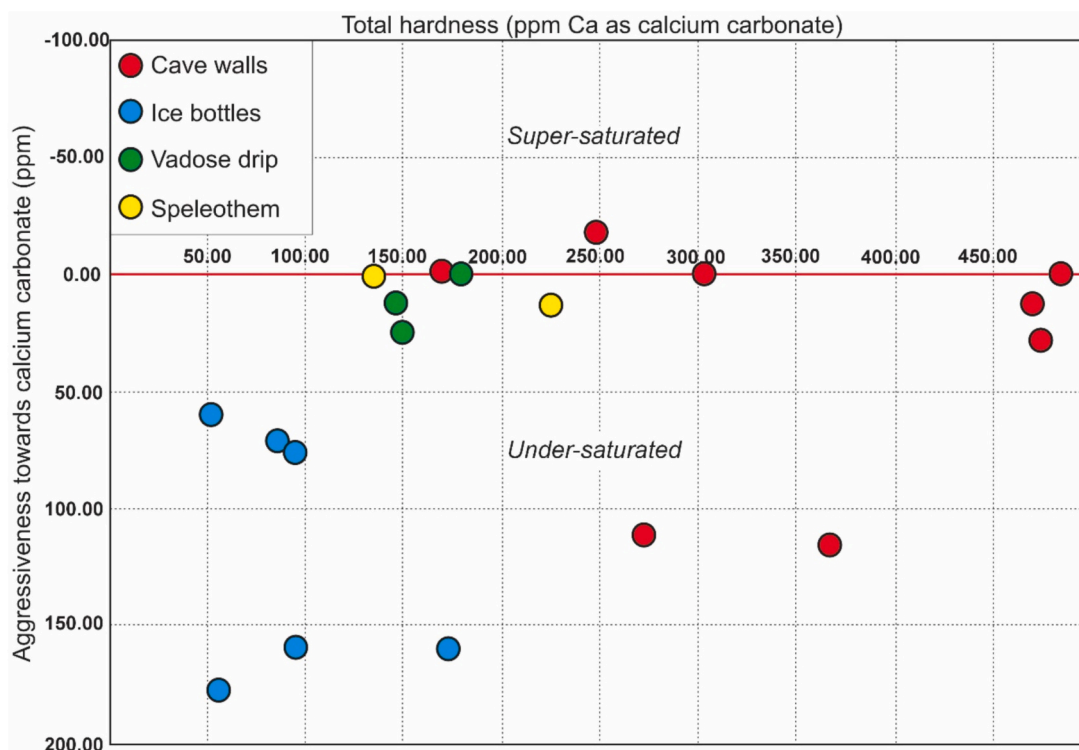


Fig. 10. Plot of Stenner aggressiveness against total hardness (as ppm CaCO_3) for various water types, indicating some wall drips are undersaturated with respect to calcium carbonate.

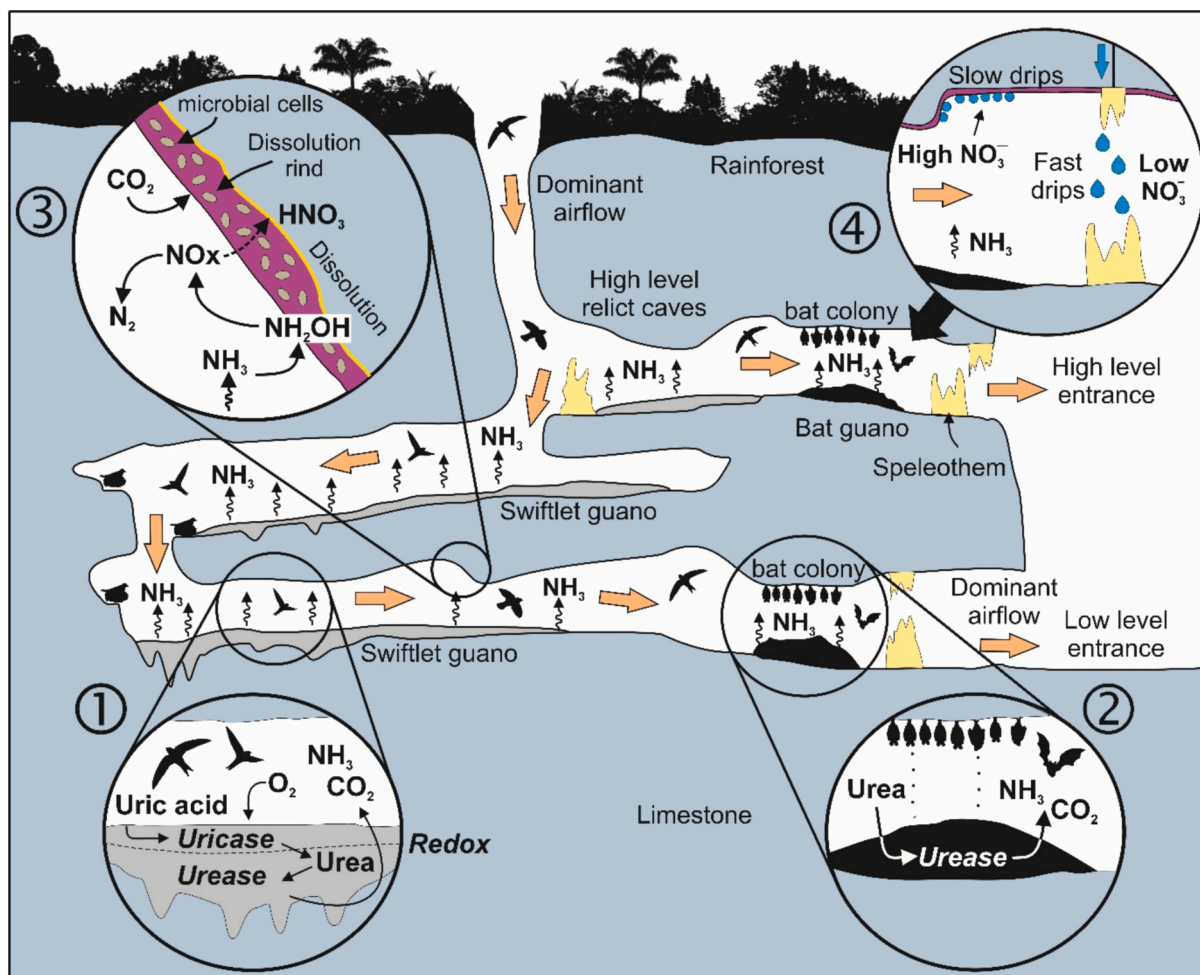


Fig. 11. Summary of processes involved in the initial production of ammonia through the decomposition of bird (1) and bat (2) guano, circulation in the cave due to air flow, which feeds the autotrophic growth of microbes on cave walls (3), causing nitrification of the ammonia, releasing NO_x , generating strong acids and causing wall rock dissolution. This results in elevated nitrate levels (4) in slow drips (condensation and percolation waters) compared to fast drips (speleothems and vadose inlets).

reflecting some uptake of ammonia from the cave air.

6.1. Production of ammonia

Bat and bird guano contain excess amounts of N. Insectivorous birds and bats are enriched in N (8–12 %) and P (2–7 %) (Misra et al., 2019). Much of this N is excreted by the animals as uric acid (birds) or urea (bats), which cannot serve as an organic source of N for growth by the microbial communities residing in these guano piles. Instead, they are broken down into bioavailable ammonia. While the breakdown of urea via urease is a common pathway in microorganisms, uric acid breakdown via the purine degradation pathway is less common. The acidic nature of both guano piles would cause any ammonia produced to remain in the sorbed ammonium phase, as the pK_a of ammonium is pH 9.3. Nonetheless, there is extensive literature on the volatilization of ammonia from animal waste, particularly as it relates to farm manure and the release of polluting levels of ammonia. Briefly, the aqueous ammonium remains highly mobile within manure (including bird feces) at low pH; however, there is a significant concentration gradient between the amount of ammonium at the surface of the manure and concentration within the air directly above (Ni, 1999). At the guano surface, even a small amount of ammonia is present which is in equilibrium with the ammonia concentration in the thin film of air directly above. As the ammonia in this thin film of air is removed by airflow it is immediately replenished from the ammonium pool. This replacement is dependent on

temperature and airflow (in accordance with Henry's Law), meaning that in warm tropical caves with significant airflow, significant quantities of ammonia are constantly released from the surface of the guano, even under low pH conditions (Ni, 1999). In support of this process, Lundberg et al. (2022) demonstrated the presence of an ammonia plume in Deer Cave associated with the large guano piles. These investigators estimated that the total flux of ammonia over 24 h was 12.26 ± 5.66 g NH_3 . We similarly detected significant ammonia concentrations of 33 mg l^{-1} above the bat guano pile in Deer Cave.

Ammonia is highly soluble in water. We believe that within the cave, ammonia is being adsorbed onto surfaces and into water vapour in the air, which then condenses out onto the walls and other surfaces with the cave (Fig. 11). Within the guano, microbial metabolic activity is powered by the considerable organic carbon found there, but on other rock surfaces within the cave, such energy is not available. Nonetheless, there is presumably significant ammonia which, under aerobic conditions, can be used by the cell as an energy source for autotrophic growth. When ammonia is used in dissimilatory reactions, ammonia is oxidized to NO_2^- (also called nitrification) and then stepwise to NO_3^- , which releases electrons that support autotrophic CO_2 fixation and growth. A significant portion of the global nitrogen cycle is driven by the autotrophic conversion of ammonia by microbial oxidation to NO_2^- and NO_3^- , which is facilitated by ammonia-oxidizing bacteria and archaea, with the formation of nitrous acid (HNO_2) and nitrogen oxides (NO_x) as intermediates during the conversion. When nitrogen oxides (NO_x), in their

gaseous forms such as nitric oxide (NO) and nitrogen dioxide (NO₂) dissolve within the surficial water, they would generate an aggressive nitric acid (HNO₃) which would in turn react with the limestone chemistry of the rock, producing calcium nitrate (Fig. 11). The aerobic conditions of these wall surfaces prevent denitrification reactions, leading to the accumulation of produced NO₃⁻, which we detected accumulating up to 6000 mg l⁻¹ in the surficial water.

7. Discussion

Dissolution by acids generated by in-situ nitrification of ammonia can explain many of the subaerial speleogens observed in the caves. The guano holes and dissolution niches are probably formed by the release of ammonia from the decaying guano which adsorbs onto adjacent bedrock surfaces (Fig. 5). This is then oxidized generating acidic byproducts. Over time a positive feedback loop develops as dissolutional enlargement makes the pit deeper, or the niche more suitable as a roosting site, which in turn favours the deposition and subsequent decomposition of additional guano and other organic detritus.

The distribution of ammonia is influenced by the strong air flow through the caves. Many of the cave passages in Mulu are very large, and many caves, including the Clearwater Cave system, have multiple entrances, some several hundred metres above the lowest entrances. Consequently, there is often strong airflow throughout the cave systems, principally due to the chimney effect resulting from the density contrast between the air inside and outside the cave. Because of the high thermal inertia of the rock, the airflow direction is typically downward during the day when the atmospheric temperature is warmer than the temperature inside the cave, reversing at night. In addition, pressure differences between cave entrances can be induced by outside wind flow, resulting in air flow through the caves. This may be significant with large cave entrances, especially those orientated in favour of surface winds. A notable example is the 100 m high entrance to Deer Cave where a strong, wind induced draught is often present.

To quantify this, we assessed air flow patterns in Racer Cave, Stone Horse Cave and Lagan's Cave by placing a WindSonic ultrasonic anemometer at a single location inside each cave, not far from the main lower entrance. Full details of the methods and results are documented in Eavis (2023). The anemometer was connected to an RPR Spacelogger, recording wind speed and bearing. Readings were taken every 4 s and data logged for several days, along with temperature, pressure and humidity. For Racer Cave, a diurnal wind cycle was observed, with typically a strong outward draught during the day and a weak or erratic inward draught at night. Peak flow volumes are about 12 m³ per second. Low atmospheric pressure (observed both inside and outside the cave) is generally, but not always, correlated with strong outward draught from the cave. In Stone Horse Cave, a similar diurnal wind cycle is seen, with typically a strong outward draught during the day and a weak or erratic inward draught at night. Peak volumes of c. 100 m³ per second during the outward phase were observed. Night-time wind speeds remained generally low. In Lagan's Cave, no clear diurnal wind cycle is seen. Instead, many oscillations between inward and outward draught, on timescales of hours to several hours, are seen. The strongest draughts are outward draughts, but there are also some strong inward draughts. Peak volumes were around 30–35 m³ per second. This additional complexity of the draught in this cave may be due to the logger's location in a complex area of interconnected passages close to multiple entrances, and large entrances either side of a hill favouring wind induced circulation. The data from all three caves shows there is a considerable flow of air through the caves, enabling a significant flux of humid air from outside. In addition, strong draughts have been noted by cavers at numerous other locations within the Mulu Caves. Any ammonia generated by microbial decay of guano will be dispersed throughout the cave system relatively quickly.

The strong airflows explains the streamlined and fluted nature of many of the dissolutional forms, as dissolution will be greatest where the

flux of ammonia is at a maximum. Once dissolution has occurred, the strong airflows can cause evaporation of the water in areas close to cave entrances or in areas of strong airflow, leading to precipitation of the dissolved carbonate and the thin carbonate paste observed on the walls. Where this paste becomes saturated following rainfall, this can cause it to be remobilised, creating the 'cockling' effect, and in some cases, globules of amorphous calcium carbonate to form on the base of bedrock pendants (Fig. 6). Degassing of the saturated drip-waters can create many small finger-type stalactites and helictites commonly observed on passage walls and ceilings.

8. Rate of dissolution and impacts on CO₂ release and carbon cycling

Evidence from the Clearwater Cave streamway suggests that passages 10–15 m above the current resurgence level have undergone sufficient dissolution to remove the primary fluvial scalloping (Fig. 2). Likewise, the absence of fluvial scallops and the generation of aerospeleogens in Racer Cave (c. 30 m above base-level), Stone Horse Cave (c. 35 m above base-level), and in Cave of the Winds (20 m above base-level) suggest the original passage morphology has been erased since the passages were abandoned by the formative river. In Lagan's Cave, just 5–10 m above the alluvial plain, the original fluvial scalloping is still present but shows clear signs of modification. The rate of base-level lowering in the Mulu caves is estimated at 19 cm per ka (Farrant et al., 1995), which suggests dissolution due to ammonia nitrification can significantly alter cave passage morphology over 10⁴-to-10⁵-year timescales. In the older, higher-level caves where this process may have been operating for hundreds of thousands, and potentially >1 million years, tens of cm to possibly metres of wall-rock retreat may have occurred, indicated by the significant corrosion of speleothems that has occurred in many parts of the cave system. This is similar to the significant level (1.7 m) of wall retreat observed by Audra et al. (2016) near bat guano piles in Morocco.

This novel speleogenetic process is likely to be spatially and temporally variable. It is most efficacious in areas where there is a significant amount of guano, in particular swiftlet guano, coupled with significant airflow and high levels of humidity. Where bat and bird guano deposits are absent, then this process will not occur. Likewise, the amount of dissolution is governed by ammonia production, which depends on the rate of guano accumulation and decomposition. Break-down of the guano varies depending on a variety of factors including temperature and moisture content. McFarlane et al. (2017) suggest that in Deer Cave, where accumulation rates of fresh bat guano are measured in millimetres per day, decomposition rates are measured in years. In the warm, moist environments present in the Mulu caves where there is a high level of microbial activity, uric acid in bird guano can degrade into ammonia relatively quickly over a period of weeks to months. The urea component in bat guano is metabolized within hours and the nitrogen volatilized as ammonia.

The dissolution of carbonate by nitric acid has potentially important implications for CO₂ release and carbon cycling in karst environments. The oxidation of ammonia, followed by dissolution of limestone by nitric acid represents a net source of CO₂ to the atmosphere (Martin, 2017), potentially affecting the karst C cycle and global climate change. This is very similar to the release of CO₂ following the application of nitrogen fertilizers on calcareous soil for agricultural purposes. This causes a decrease in riverine alkalinity and a net release of CO₂ to the atmosphere due to the substitution of carbonic acid by protons produced by nitrification of N-fertilizers occurring in soils (Perrin et al., 2008).

9. Conclusions

The widespread occurrence of bats and swiftlets in caves across southeast Asia and in other tropical and warm temperate regions suggests this process is likely to be commonplace. Many caves that host bat

and swiftlet populations are likely to show evidence of biogenic corrosion due to ammonia nitrification. In Sarawak, other examples include the Gomantong caves (Lundberg and McFarlane, 2012), Niah Cave (Harrisson and Medway, 1959), and the Bau caves near Kuching in western Sarawak (Wurster et al., 2017). These all have biogenic passage morphologies similar to those seen in Mulu. Tropical and warm temperate caves across the globe show similar morphologies which we attribute, at least in part, to biogenic dissolution by nitrification. These include Chameau Cave, Morocco (Audra et al., 2021), Natuturingam Cave, Philippines (Calaforra et al., 2022); the Domic, Drienovská and Jasovská caves in south-eastern Slovakia (Sala et al., 2023), caves in the Kyrenia range, Cyprus (Cailhol et al., 2019), Roquette cave, Gard, France (Bruxelles et al., 2022), Drotsky's Cave, NW Botswana (Dandurand et al., 2019) and some caves in Australia (Dwyer, 1965). The impacts of this process may be related to ammonia release from guano, which is dictated by temperature and airflow (per Henry's Law). The size of the passage could also play an important role, with larger passages allowing ammonia-rich air to flow further before being adsorbed onto surfaces. The adsorption of ammonia may also be influenced by humidity and condensation. In poorly ventilated caves, gas dispersion is limited, any biocorrosion is likely to be more localised around the source of ammonia. Additional work should therefore consider passage size, temperature, humidity, and airflow when interpreting the presence of megascallops and other ammonia-driven dissolution features.

The novel speleogenetic mechanism identified in this work may have profound implications for how caves are interpreted. Cave passage morphology is one of the most valuable features to understand and interpret modes of cave formation, and by implication, elicit landscape and environmental change (Palmer, 2007). Many of the features observed in the Mulu caves have previously been ascribed to deep phreatic processes (Brook and Waltham, 1978; Waltham and Brook, 1980; Worthington, 2004) on the basis of the large, presumed phreatic megascallops, or paragenetic development beneath a sediment fill now removed (Farrant and Smart, 2011). The recognition of a characteristic morphological suite of biogenic corrosion has led to a reassessment of the evolution of the Mulu cave systems and attendant landscape development. The Mulu caves are no longer considered to be predominantly deep phreatic systems, but instead comprise shallow phreatic and vadose passages developed along strike with some deep phreatic loops where passages are aligned down dip, with local paragenetic modification. A similar reassessment may be needed for many other tropical caves. Biogenic corrosion and augmented condensation corrosion and should be considered when interpreting caves that have bat or swiftlet populations.

CRedit authorship contribution statement

Andrew R. Farrant: Writing – review & editing, Writing – original draft, Supervision, Project administration, Methodology, Investigation, Conceptualization. **J. Max Koether:** Writing – original draft, Investigation, Formal analysis. **Hazel A. Barton:** Writing – review & editing, Writing – original draft, Supervision, Project administration, Methodology, Investigation, Formal analysis, Conceptualization. **Stein-Erik Lauritzen:** Writing – original draft, Methodology, Investigation, Formal analysis. **Christos Pennos:** Writing – original draft, Investigation, Formal analysis. **Andrew C. Smith:** Writing – review & editing, Methodology, Investigation, Conceptualization. **Jo White:** Writing – original draft, Investigation. **Andrew McLeod:** Writing – review & editing, Investigation. **Andrew J. Eavis:** Supervision, Investigation, Funding acquisition.

Declaration of competing interest

The authors declare the following financial interests/personal relationships which may be considered as potential competing interests:

Andrew Farrant reports limited administrative support and travel were provided by the Mulu Caves Project. If there are other authors, they declare that they have no known competing financial interests or personal relationships that could have appeared to influence the work reported in this paper.

Acknowledgements

This research would not have been possible without the help and assistance of The Mulu Caves Project, a collaboration between speleologists (mostly from the UK) and the Sarawak Authorities, particularly the Sarawak Forestry Corporation, working in association with Gunung Mulu National Park management and staff. We would like to thank the staff at the Gunung Mulu National Park, and in particular Rambli Ahmad (Sarawak Forestry Corporation), Hein Gerstner (Manager at Borsarmulu National Park & Heritage), Mark Kuneiglibuan Tisen (Park Warden), Venio Enar, and the late David Gill, former Park Development Officer who sadly passed away before this paper was published. Permission to undertake research and collect samples was granted by the Sarawak Forestry Corporation. We thank the reviewers for insightful reviews. Peter Smart is thanked for stimulating early work on cave geomorphology and the biogenic crusts, while Andrew Marriot is thanked for providing some of the water chemistry data. Research funding was provided in part by the University of Alabama Graduate School and the Department of Geological Sciences through the CRF (Conference and Research Funding) award. Farrant and Smith publish with the approval of the Executive Director, British Geological Survey.

Data availability

Data will be made available on request.

References

- Audra, P., Barriquand, L., Bigot, J.Y., Cailhol, D., Caillaud, H., Vanara, N., Nobécourt, J. C., Madonia, G., Vattano, M., Renda, M., 2016. L'impact méconnu des chauves-souris et du guano dans l'évolution morphologique tardive des cavernes. *Karstologia* 68, 1–20.
- Audra, P., De Waele, J., Bentaleb, I., Chroňáková, A., Kristúfek, V., D'Angeli, I.M., Carbone, C., Madonia, G., Vattano, M., Scopelliti, G., Cailhol, D., Vanara, N., Temovski, M., Bigot, J.Y., Nobécourt, J.C., Galli, E., Rull, F., Sanz-Arranz, A., 2019. Guano-related phosphates-rich minerals in European caves. *Int. J. Speleol.* 48, 75–105.
- Audra, P., Heresanu, V., Barriquand, L., Boutchich, M.E.K., Jailet, S., Pons-Branchu, E., Bosák, P., Cheng, H., Edwards, R.L., Renda, M., 2021. Bat guano minerals and mineralization processes in Chameau Cave, Eastern Morocco. *Int. J. Speleol.* 50, 91–109.
- Barriquand, L., Bigot, J.-Y., Audra, P., Cailhol, D., Gauchon, C., Heresanu, V., Jailet, S., Vanara, N., 2021. Caves and bats: morphological impacts and archaeological implications. The azé prehistoric cave (Saône-et-Loire, France). *Geomorphology* 388, 107785.
- Barton, H.A., Jurado, V., 2007. What's up down there? Microbial diversity in caves. *Microbe* 2, 132–138.
- Barton, H.A., Northup, D.E., 2007. Geomicrobiology in cave environments: past, current, and future perspectives. *J. Cave Karst Stud.* 69, 163–178.
- Barton, H.A., Taylor, N.M., Lubbers, B.R., Pemberton, A.C., 2006. DNA extraction from low-biomass carbonate rock: an improved method with reduced contamination and the low-biomass contaminant database. *J. Microbiol. Methods* 66, 21–31.
- Bird, M.I., Boobyer, E.M., Bryant, C., Lewis, H.A., Paz, V., Stephens, W.E., 2007. A long record of environmental change from bat guano deposits in Makangit Cave, Palawan, Philippines. *Earth Environ. Sci. Trans. R. Soc. Edinb.* 98, 59–69.
- Blumberg, P.N., Curl, R.L., 1974. Experimental and theoretical studies of dissolution roughness. *J. Fluid Mech.* 65, 735–751.
- Bokhorst, S., van Logtestijn, R., Convey, P., Aerts, R., 2019. Nitrogen isotope fractionation explains the 15 N enrichment of Antarctic cryptogams by volatilized ammonia from penguin and seal colonies. *Polar Res.* 38, 3355.
- Brook, D.B., Waltham, A.C., 1978. The Limestone Caves of Gunung Mulu National Park, Sarawak. Royal Geographical Society, London (44 pp.).
- Bruxelles, L., Barriquand, L., Bigot, J.-Y., Cailhol, D., Genuite, K., Jailet, S., 2022. Origin of the asymmetry of certain fossil galleries: the major role of biocorrosion as exemplified in the Roquette cave (Gard, France). In: *Karstologia Mémoires, 18th International Congress of Speleology-Savoie, Mont Blanc, vol. 4*, pp. 305–308.
- Bushuk, M., Holland, D.M., Stanton, T.P., Stern, A., Gray, C., 2019. Ice scallops: a laboratory investigation of the ice-water interface. *J. Fluid Mech.* 873, 942–976.

- Busquets, A., Fornós, J.J., Zafra, F., Lalucat, J., Merino, A., 2014. Microbial communities in a coastal cave: Cova des Pas de Vallgornera (Mallorca, Western Mediterranean). *Int. J. Speleol.* 43, 205–216.
- Butler, D.R., 1995. *Zoogeomorphology: Animals as Geomorphic Agents*. Cambridge University Press (240 pp.).
- Cailhol, D., Audra, P., Nehme, C., Nader, F.H., Garašić, M., Heresanu, V., Guceľ, S., Charalambidou, I., Satterfield, L., Cheng, H., Edwards, L., 2019. The contribution of condensation-corrosion in the morphological evolution of caves in semi-arid regions: preliminary investigations in the Kyrenia range, Cyprus. *Acta Carsol.* 48, 5–27.
- Caillaud, H., 2017. *Zoogeomorphologie: les chiroptères comme facteurs géomorphologiques des paysages souterrains*. Université Paris 1 Panthéon-Sorbonne, Mémoire de master 2 de géographie, Paris.
- Calaforra, J.M., De Waele, J., Forti, P., Santagata, T., Vattano, M., 2019. The guano holes: a new corrosion form from Natuturingam Cave (Palawan, Philippines). *Trav. Inst. Speol. E. Racovitza* 47, 35–47.
- Calaforra, J.M., De Waele, J., Forti, P., Gázquez, F., Santagata, T., Vattano, M., 2022. The guano holes and guano pots: two new climate-controlled biogenic corrosion forms in Puerto Princesa karst area (Palawan, Philippines). In: 18th International Congress of Speleology-Savoie Mont Blanc 2022, Vol. IV-Karstologia Mémoires n° 24.
- Dandurand, G., Duranthon, F., Jarry, M., Stratford, D.J., Bruxelles, L., 2019. Biogenic corrosion caused by bats in Drotsky's Cave (the Gcwhaba Hills, NW Botswana). *Geomorphology* 327, 284–296.
- DuChene, H.R., Palmer, A.N., Palmer, M.V., Michael Queen, J., Polyak, V.J., Decker, D. D., Hill, C.A., Spilde, M., Burger, P.A., Kirkland, D.W., Boston, P., 2017. Hypogene speleogenesis in the Guadalupe Mountains, New Mexico and Texas, USA. In: *Hypogene Karst Regions and Caves of the World*, pp. 511–530.
- Dwyer, P.D., 1965. Bat erosion in Australian limestone caves. *Helictite* 3, 85–90.
- Eavis, R., 2023. Report on the findings of the Mulu Caves Project Expedition to the Gunung Mulu National Park, Sarawak. In: *Mulu Caves 2022 Expedition Report. The Mulu Caves Project* (90 pp.).
- Farnleitner, A.H., Wilhartitz, I., Ryzinska, G., Kirschnner, A.K., Stadler, H., Burtscher, M. M., Hornek, R., Szewzyk, U., Herndl, G., Mach, R.L., 2005. Bacterial dynamics in spring water of alpine karst aquifers indicates the presence of stable autochthonous microbial endokarst communities. *Environ. Microbiol.* 7, 1248–1259.
- Farrant, A.R., Smart, P.L., 2011. Role of sediment in speleogenesis; sedimentation and paragenesis. *Geomorphology* 134, 79–93.
- Farrant, A.R., Smart, P.L., Whitaker, F.F., Tarling, D.H., 1995. Long-term Quaternary uplift rates inferred from limestone caves in Sarawak, Malaysia. *Geology* 23, 357–360.
- Farrant, A.R., Kirby, M., Smart, P.L., 2007. The caves of Mulu, Sarawak: their exploration and geomorphology. *Cave Karst Sci.* 34, 51–60.
- Ford, D.C., Williams, P.D., 2007. *Karst Hydrogeology and Geomorphology*. John Wiley & Sons.
- Frank, D.A., Evans, R.D., Tracy, B.F., 2004. The role of ammonia volatilization in controlling the natural ^{15}N abundance of a grazed grassland. *Biogeochemistry* 68, 169–178.
- Goldie, H.S., 2005. Erratic judgements: re-evaluating solutional erosion rates of limestones using erratic-pedestal sites, including Norber, Yorkshire. *Area* 37, 433–442.
- Harrison, T., Medway, 1959. 'Bat Erosion' at Niah Great Caves. *Nature* 183, 971.
- James, D.M.D., 1984. *The Geology and Hydro-carbon Resources of Negara Brunei Darussalam*. Brunei Museum and Brunei Shell Petroleum Company (164 pp.).
- James, J.M., 2011. The enigma of bellholes. *Australas. Cave Karst Manag. Australas. J.* 19, 232–241.
- Jones, D.S., Northup, D.E., 2021. Cave decorating with microbes: geomicrobiology of caves. *Elements* 17, 107–112.
- Kim, Y.J., Choi, W.J., Lim, S.S., Kwak, J.H., Chang, S.X., Kim, H.Y., Yoon, K.S., Ro, H.M., 2008. Changes in nitrogen isotopic compositions during composting of cattle feedlot manure: effects of bedding material type. *Bioresour. Technol.* 99, 5452–5458.
- Klimchouk, A.B., 2009. Morphogenesis of hypogenic caves. *Geomorphology* 106, 100–117.
- Lauritzen, S.-E., 1981. A study of some karst waters in Norway. Spatial variation in solute concentrations and equilibrium parameters in limestone dissolution. *Nor. Geogr. Tidsskr.* 35, 1–19.
- Lauritzen, S.-E., 1982. The paleocurrents and morphology of Pikhaggrottene, Svartisen, North Norway. *Nor. Geogr. Tidsskr.* 36, 183–209.
- Lundberg, J., McFarlane, D.A., 2009. Bats and bell holes: the microclimatic impact of bat roosting, using a case study from Runaway Bay Caves, Jamaica. *Geomorphology* 106, 78–85. <https://doi.org/10.1016/j.geomorph.2008.09.022>.
- Lundberg, J., McFarlane, D.A., 2012. Post-speleogenetic biogenic modification of Gomantong Caves, Sabah, Borneo. *Geomorphology* 157, 153–158.
- Lundberg, J., McFarlane, D.A., Van Rentergem, G., 2022. The nitrogen dynamics of Deer Cave, Sarawak, and the role of bat caves as biogeochemical sinks in Tropical Moist Forests. *Int. J. Speleol.* 51, 205–221.
- Martin, J.B., 2017. Carbonate minerals in the global carbon cycle. *Chem. Geol.* 449, 58–72. <https://doi.org/10.1016/j.chemgeo.2016.11.029>.
- McFarlane, D.A., Keeler, R.-C., Mizutani, H., 1995. Ammonia volatilization in a Mexican bat cave ecosystem. *Biogeochemistry* 30, 1–8.
- McFarlane, D.A., Lundberg, J., van Rentergem, G., 2017. Preliminary observations on tropical bat caves as biogeochemical nitrogen sinks. In: *Proceedings of the 17th International Congress of Speleology*, Vol. 1, pp. 157–161.
- Misra, P.K., Gautam, N.K., Elangovan, V., 2019. Bat guano: a rich source of macro and microelements essential for plant growth. *Ann. Plant Soil Res.* 21, 82–86.
- Moseley, G.E., Richards, D.A., Smith, C., Smart, P.L., Hoffman, D.L., Farrant, A.R., 2013. U-Th dating of speleothems to investigate the evolution of limestone caves in the Gunung Mulu National Park, Sarawak, Malaysia. *Cave Karst Sci.* 40, 13–16.
- Newton, R.J., Jones, S.E., Eiler, A., McMahon, K.D., Bertilsson, S., 2011. A guide to the natural history of freshwater lake bacteria. *Microbiol. Mol. Biol. Rev.* 75 (1), 14–49.
- Ni, J., 1999. Mechanistic models of ammonia release from liquid manure: a review. *J. Agric. Eng. Res.* 72, 1–17.
- Palmer, A.N., 2007. *Cave Geology*. Cave Books (454 pp.).
- Perrin, A.S., Probst, A., Probst, J.L., 2008. Impact of nitrogenous fertilizers on carbonate dissolution in small agricultural catchments: implications for weathering CO_2 uptake at regional and global scales. *Geochim. Cosmochim. Acta* 72, 3105–3123.
- Plan, L., Tschegg, C., De Waele, J., Spötl, C., 2012. Corrosion morphology and cave wall alteration in an Alpine sulfuric acid cave (Kraushöhle, Austria). *Geomorphology* 169, 45–54.
- Sala, P., Bella, P., Postawa, T., Wróblewski, W., Gradziński, M., 2023. Corrosion of carbonate speleothems by bat guano. *Sediment. Geol.* 106454.
- Sebilo, M., Aloisi, G., Mayer, B., Perrin, E., Vaury, V., Mothet, A., Laverman, A.M., 2019. Controls on the isotopic composition of nitrite ($\delta^{15}\text{N}$ and $\delta^{18}\text{O}$) during denitrification in freshwater sediments. *Sci. Rep.* 9, 19206.
- Smart, P.L., Bull, P.A., Rose, J., Laverty, M., Friederich, H., Noel, M., 1985. Surface and underground fluvial activity in the Gunung Mulu National Park, Sarawak. In: Douglas, I., Spencer, T. (Eds.), *Environmental Change and Tropical Geomorphology*. Routledge, pp. 123–148.
- Smith, R.J., Jeffries, T.C., Roudnew, B., Fitch, A.J., Seymour, J.R., Delpin, M.W., Newton, K., Brown, M.H., Mitchell, J.G., 2012. Metagenomic comparison of microbial communities inhabiting confined and unconfined aquifer ecosystems. *Environ. Microbiol.* 14, 240–253.
- St. Lawrence, H. (Ed.), 2015. *Mulu Caves 2014 Expedition Report. Mulu Caves Project* (114 pp.).
- Stenner, R.D., 1969. The measurement of the aggressiveness of water towards calcium carbonate. *Trans. Cave Res. Group Great Britain* 11, 175–200.
- Tarhule-Lips, R.F., Ford, D.C., 1998. Condensation corrosion in caves on Cayman Brac and Isla de Mona. *J. Cave Karst Stud.* 60, 84–95.
- Viles, H.A., 2012. Microbial geomorphology: a neglected link between life and landscape. *Geomorphology* 157, 6–16.
- Viles, H., 2020. Biogeomorphology: past, present and future. *Geomorphology* 366, 106809.
- Waltham, A.C., Brook, D.B., 1980. Geomorphological observations in the limestone caves of the Gunung Mulu National Park, Sarawak. *Br. Cave Res. Assoc. Trans.* 7, 123–139.
- Wannier, M., 2009. Carbonate platforms in wedge-top basins: an example from the Gunung Mulu National Park, Northern Sarawak (Malaysia). *Mar. Pet. Geol.* 26 (2), 177–207.
- Wigley, T.M.L., Brown, M.C., 1971. Geophysical applications of heat and mass transfer in turbulent pipe flow. *Bound.-Layer Meteorol.* 1, 300–320.
- Worthington, S.R., 2004. Hydraulic and geological factors influencing conduit flow depth. *Cave Karst Sci.* 31, 123–134.
- Wurster, C.M., Munksgaard, N., Zwart, C., Bird, M., 2015. The biogeochemistry of insectivorous cave guano: a case study from insular Southeast Asia. *Biogeochemistry* 124, 163–175. <https://doi.org/10.1007/s10533-015-0089-0>.
- Wurster, C.M., Rifai, H., Haig, J., Titin, J., Jacobsen, G., Bird, M., 2017. Stable isotope composition of cave guano from eastern Borneo reveals tropical environments over the past 15,000 cal yr BP. *Palaeogeogr. Palaeoclimatol. Palaeoecol.* 473, 73–81.